Copepod Grazing Influences Diatom Aggregation and Particle Dynamics

Jordan Toullec[1], Dorothée Vincent[2,3], Laura Frohn[1], Philippe Miner[4], Manon Le Goff[1], Jérémy Devesa[1] and Brivaëla Moriceau[1]*

[1] Univ Brest, CNRS, IRD, Ifremer, LEMAR, Plouzané, France, [2] UMR 8187 Laboratoire d'Océanologie et de Géosciences, CNRS, Université du Littoral-Côte d'Opale, Wimereux, France, [3] Agence Française pour la Biodiversité, Direction de l'Appui aux Politiques et aux Acteurs, Service Connaissance, Evaluation et Surveillance du Milieu Marin, Espace Giraudeau, Brest, France, [4] Ifremer, Univ Brest, CNRS, IRD, LEMAR, Plouzané, France

In marine ecosystems, carbon export is driven by particle flux which is modulated by aggregation, remineralization, and grazing processes. Zooplankton contribute to the sinking flux through the egestion of fast sinking fecal pellets but may also attenuate the flux by tearing apart phytoplankton aggregates into small pieces through swimming activity or direct ingestion. Freely suspended cells, artificial monospecific aggregates from two different diatom species (*Chaetoceros neogracile* and *Skeletonema marinoi*) and natural aggregates of *Melosira* sp. were independently incubated with five different copepod species (*Acartia clausi*, *Temora longicornis*, *Calanus helgolandicus*, *Euterpina acutifrons*, and *Calanus hyperboreus*). During the grazing experiments initiated with free diatoms, *E. acutifrons* feeding activity evidenced by ingestion rates of 157 ± 155 ng Chl a ind^{-1} d^{-1}, induced a significant increase of *S. marinoi* aggregation. Transparent exopolymeric particles (TEP) production was only slightly boosted by the presence of grazers and turbulences created by swimming may be the main trigger of the aggregation processes. All copepods studied were able to graze on aggregates and quantitative estimates led to chlorophyll a ingestion rates (expressed in Chla a equivalent, i.e., the sum of chlorophyll *a* and pheopigments in their guts) ranging from 4 to 23 ng Chl a$_{eq}$ ind^{-1} d^{-1}. The relation between equivalent spherical diameters (ESDs) and sinking velocities of the aggregates did not significantly change after grazing, suggesting that copepod grazing did not affect aggregate density as also shown by Si:C and C:N ratios. Three main trends in particle dynamics could be identified and further linked to the copepod feeding behavior and the size ratio between prey and predators: (1) Fragmentation of *S. marinoi* aggregates by the cruise feeder *T. longicornis* and of *Melosira* sp. aggregates by *C. hyperboreus* at prey to predator size ratios larger than 15; (2) no change of particle dynamics in the presence of the detritic cruise feeder *E. acutifrons*; and finally (3) re-aggregation of *C. neogracile* and *S. marinoi* aggregates when the two filter feeders *A. clausi* and *C. helgolandicus* were grazing on aggregate at prey to predator size ratios lower than 10. Aggregation of freely suspended cells or small aggregates was facilitated by turbulence resulting from active swimming of small copepods. However, stronger turbulence created by larger cruise feeders copepods prevent aggregate formation and even made them vulnerable to breakage.

Keywords: diatom aggregate, grazing experiment, copepod, sinking velocity, particle dynamics

INTRODUCTION

In marine ecosystems, diatoms play a key role in the biological carbon pump (Jin et al., 2006; Tréguer et al., 2017). Diatom contribution to the export is mainly driven by particle dynamics such as aggregate formation, by coagulation of freely suspended phytoplankton cells or small detritus into a sticky matrix made of transparent exopolymeric particles (TEPs). Considering the balance between sinking and remineralization, only large and fast sinking particles formed in the mixed layer can reach the sequestration depth (Moriceau et al., 2007), i.e., 1000 m depth considering that an efficient carbon entrapment is longer than a thousand year (Passow and Carlson, 2012). This mechanistic view is confirmed by *in situ* profiles of particle fluxes (Guidi et al., 2007). Yet, viable freely suspended cells were collected at depth down to 4000 m (Agustí et al., 2015). Due to their slow sinking rates (1–5 m d^{-1}, Bienfang, 1981) isolated living cells cannot reach water layer as deep. Living cells may require transportation to depth *via* aggregates and then dispersed after disaggregation of the fast sinking particle by unknown processes. Strong decrease of the particle size with depth confirm the attenuation of particle fluxes under the mixed layer depth (Guidi et al., 2007). From *in situ* observations in the NW Mediterranean Sea, Stemmann et al. (2004) proposed different processes possibly explaining fragmentation of sinking particles, namely microbial activity and zooplankton feeding. Zooplankton grazers can strongly modulate the particle fluxes in the water column. Organisms such as salps, appendicularians, and copepods are acknowledged to be important contributors to carbon export *via* the production of fast sinking fecal pellets resulting from grazing (Stemmann et al., 2002; Turner, 2002, 2015; Boyd and Trull, 2007; Stamieszkin et al., 2015; Lalande et al., 2016). Overall, the contribution of fecal pellets to the total particle carbon flux varies from 1 to 100%, most values being <40% (Turner, 2015). In addition, during vertical migrations, zooplankton egest fecal pellets deeper than the mixed layer (Wilson et al., 2008; Brierley, 2014) resulting in an active transport of fresh organic matter at depth (Gorgues et al., 2019) as observed in the Scotia Sea and the Southern Ocean (Cavan et al., 2015, 2017; Bode et al., 2018). As a consequence, a significant proportion of the particle flux may escape remineralization processes in the upper pelagic zone (Cavan et al., 2015). Additional metabolic processes such as respiration and excretion occurring deeper during zooplankton migration also contribute to transport dissolved carbon to the deep sea (Turner, 2015; Steinberg and Landry, 2017; Hernández-León et al., 2019). Direct relation between increasing carbon export and copepod abundance was evidenced *in situ* in Kongsfjorden (Norway, Lalande et al., 2016) when diatoms dominate the community as well as during a mesocosm study conducted in the Bay of Hopavagen (Norway, Moriceau et al., 2018). However, in the latter case, this increase in carbon export was only visible when cyanobacteria (and not diatoms) dominated the phytoplankton community. Other zooplankton organisms, such as appendicularians, are major contributors to vertical particle carbon flux (Alldredge et al., 2005), *via* the production of cellulosic houses embedded with detritus or other plankton organisms (Gorsky et al., 1999;

Vargas et al., 2002; Lombard and Kiørboe, 2010; Lombard et al., 2013a).

Moreover, zooplankton may also attenuate vertical particle fluxes through different activities. Swimming of large Euphausiids was demonstrated to fragment marine aggregates into small particles that sink more slowly, become accessible to small grazers and microbial organisms, thus enhancing remineralization and carbon cycling (Dilling and Alldredge, 2000; Goldthwait et al., 2004, 2005). Sinking organic materials such as marine snow aggregates and fecal pellets could also constitute alternative food sources for mesozooplankton (Dagg, 1993; Lampitt et al., 1993; Steinberg, 1995; Dilling et al., 1998; Kiørboe, 2000; Dilling and Brzezinski, 2004; Koski et al., 2017). Ostracods, cladocerans, ascidian larvae, and copepods are aggregate colonizers, and can feed either on prokaryotic community located inside or at the surface of the aggregates, or directly on the aggregate matrix (Green and Dagg, 1997; Shanks and Walters, 1997). From 20 to 70% of the aggregate carbon biomass may be degraded by these colonizers during their sinking under the euphotic zone (Kiørboe, 2000). In a recent study investigating copepod grazing behavior on aggregated particles, Koski et al. (2017) demonstrated that both harpacticoida and poecilostomatoida copepods were able to feed on aggregates and could thus attenuate the particle carbon flux. Aggregation processes and dynamics are increasingly understood *via* the combination of laboratory experiments and models (Beauvais et al., 2006; Passow and De La Rocha, 2006; Gärdes et al., 2011; Jackson, 2015; Prairie et al., 2019), mesocosm experiments (Alldredge et al., 1995; Passow and Alldredge, 1995b; Svensen et al., 2001, 2002; Moriceau et al., 2018; Cisternas-Novoa et al., 2019), and *in situ* observations (Lampitt et al., 2010; Laurenceau-Cornec et al., 2015; Nowald et al., 2015; Giering et al., 2017; Cavan et al., 2018; Bach et al., 2019). In the meantime, studies focusing on disaggregation processes due to remineralization or zooplankton activity (Goldthwait et al., 2004; Taucher et al., 2018) remain limited despite their importance in providing new insights to better understand particle export in the mesopelagic zone. As dominant components of zooplankton communities, copepods may be considered as "gatekeepers of the biological carbon pump" if they limit carbon export by breaking aggregates as previously suggested in laboratory (Goldthwait et al., 2004), mesocosm experiments (Moriceau et al., 2018; Taucher et al., 2018), and *in situ* studies (Dilling and Alldredge, 2000). They may also enhance carbon export by (1) egesting large sinking fecal pellets (Turner, 2015; Lalande et al., 2016; Steinberg and Landry, 2017), (2) boosting the aggregation, as seen for cyanobacteria, appendicularians, and doliolids (Moriceau et al., 2018; Taucher et al., 2018), and (3) increasing the particle sinking rates when increasing the silicon content of diatoms (Pondaven et al., 2007). Swimming activity being intrinsically linked to feeding, copepod flexible diet may also modulate particle fluxes through differential grazing between free diatoms and aggregated diatoms (Bochdansky and Herndl, 1992; Bochdansky et al., 1995) or by changing the composition of the phytoplankton community (Bach et al., 2019). Their distinct functional feeding traits as filter feeders or ambush feeders

(Kiørboe, 2011; Lombard et al., 2013b; Koski et al., 2017) make them organisms of particular interest to study particle dynamics. Recognizing that only very few studies have dealt with the interactions between large particles and grazers under laboratory conditions, we propose here to study the effects of both copepod grazing and swimming activities on diatom aggregate dynamics (i.e., changes in size, sinking velocity, and elemental composition) using rolling tank experiments (Shanks and Edmondson, 1989).

MATERIALS AND METHODS

Experimental Set-Up

Two types of incubation experiments were carried out to estimate the effect of copepod grazing on particle dynamics. The first set of experiments tested whether copepod activities influence coagulation rate of free diatoms and/or the size, sinking velocity, and composition of the resulting aggregates (Experiments 1–3). The second set of experiments monitored the changes in diatom aggregate abundance, size, sinking velocity, and composition under grazing pressure (Experiments 4–8; **Figure 1**). Aggregates studied here were visible to the naked eyes starting in length from 1 mm.

Phytoplankton Cultures

For laboratory experiments (Experiments 1–7), *Skeletonema marinoi* (strain CCAP 1077/5) and *Chaetoceros neogracile* (strain CCAP 1010/3) were obtained from Ifremer collection (Laboratory of Functional Physiology of Marine Organism, Ifremer Brittany's Centre, France). They were continuously grown in Conway medium (Conway et al., 1976) prepared with autoclaved 1 µm filtered seawater from the Bay of Brest (Brittany, France). Cells were maintained in exponential growth phase in 2 L glass round bottom balloons at 20°C under continuous irradiance (100 µmoles photons m^{-2} s^{-1}). Balloons were kept in constant aeration and CO_2 was supplied to keep the pH between 7.5 and 7.9. These cultures were directly used for experiments using free diatom cells as prey type (Experiments 1–3, **Table 1**). Subsamples of the cultures were used for chemical analyses at T_{init} (see below).

Aggregate Preparation From Diatom Cultures and *in situ* Aggregate Collection
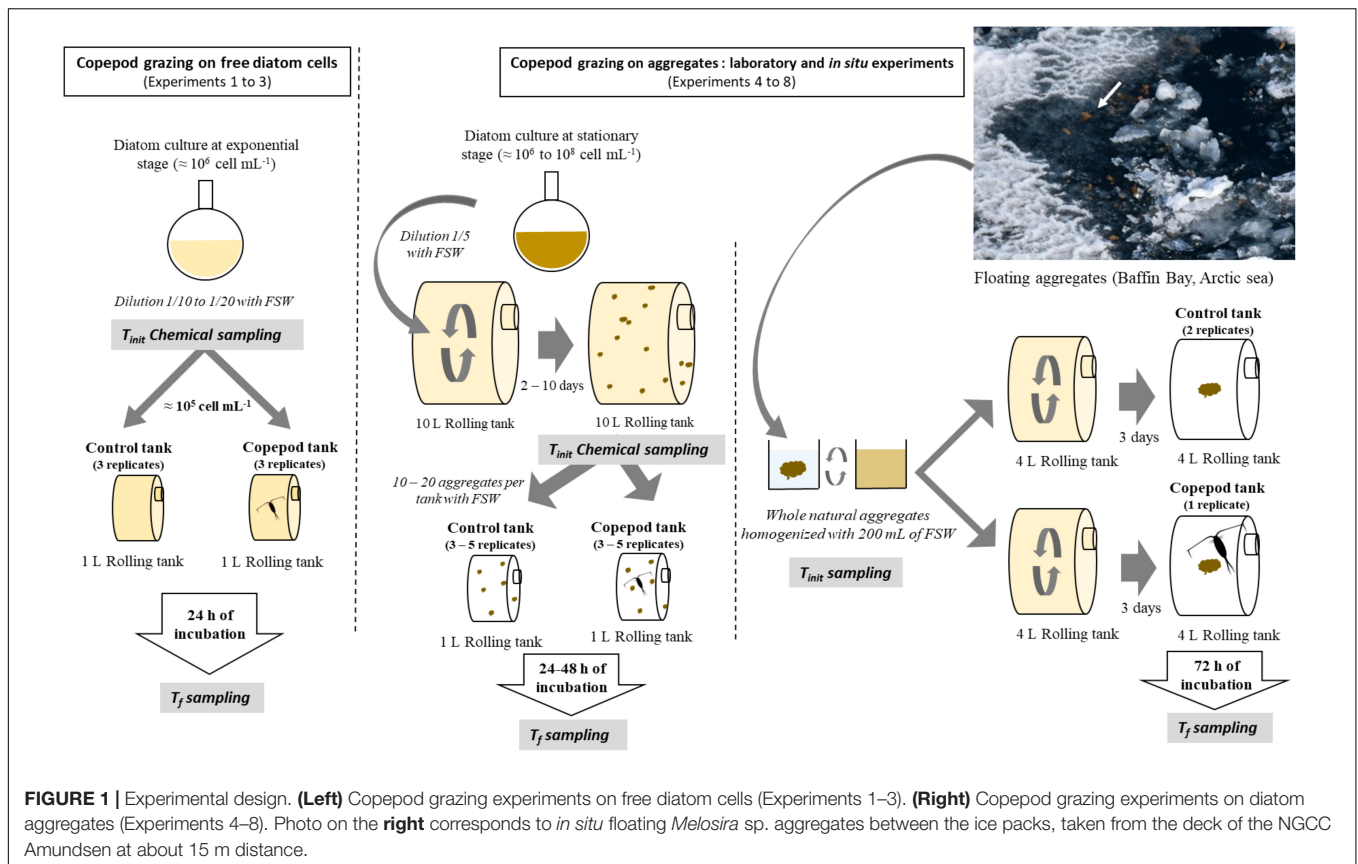
In order to perform Experiments 4–8, monospecific aggregates were produced in the laboratory. Once diatom cultures reached the stationary phase, i.e., stable cell concentrations of 10^6–10^7 for *S. marinoi* and 10^8 cell mL^{-1} for *C. neogracile*, 2 L were diluted into 10 L cylindrical rolling tanks containing 1 µm filtered UV sterilized seawater (FSW hereafter, **Figure 1**). Cultures were then maintained at 18°C under a 12:12 h photoperiod cycle, for 2–10 days, and rotated at 3 rpm on a rolling table to promote cell collision and aggregation (Shanks and Edmondson, 1989). As soon as aggregates were formed inside the 10 L rolling tank, 10–20 aggregates were carefully transferred inside a set of 1 L rolling tanks containing FSW using a large aperture plastic pipette (10 mL). Similar sampling was done to measure the initial chemical conditions (T_{init}) of the aggregates (see below).

For the *in situ* experiment (Experiment 8), large floating mono-specific aggregates of *Melosira* sp. were sampled from the surface from a zodiac boat on the 3rd of July 2016 during the GreenEdge expedition on-board the NGCC Amundsen. The aggregates were sampled at station 600 (70°30.653 N, 63°59.258 W) using a 0.1 mm mesh sieve (**Figure 1**). *Melosira* sp. aggregates were diluted into 200 mL of 0.7 µm FSW sampled with a Niskin bottle at 50 m depth (salinity 32.7, T^0 −1.5°C). The mixture was homogenized and divided into four aliquots. The first aliquot was kept for biogeochemical analyses [particulate organic carbon (POC)/nitrogen (PON) and $bSiO_2$ content] and for taxonomic analysis of phytoplankton. The three other aliquots were distributed into three rolling tanks (4 L) containing *in situ* 0.7 µm FSW. Rolling tanks were stored in the dark in a cold room (4°C) and rotated on a rolling table at 3.3 rpm. This incubation ended up in the formation of a large aggregate (26.8–34 mm, **Figure 1**).

Copepod Sampling and Rearing Phase

Four copepod species (*Euterpina acutifrons*, *Temora longicornis*, *Acartia clausi*, and *Calanus helgolandicus*) were selected for the laboratory experiments on diatom free cells and aggregates (**Tables 1**, **2**). They were chosen for their easiness of cultivation, as their presence generally matches phytoplankton spring blooms in the area (Schultes et al., 2013), and because they display different functional traits (Benedetti et al., 2015) regarding feeding strategies and sizes. *A. clausi* (0.9 mm total length) and *C. helgolandicus* (2.7 mm total length) are both omnivorous filter feeders with a clear tendency to herbivory, the latter being able to migrate vertically (Andersen et al., 2001, 2004). *T. longicornis* (0.8 mm total length) and *E. acutifrons* (0.5 mm total length) are described as cruise feeders (Lombard et al., 2013b), *E. acutifrons* having the tendency to feed on detrital matter (Benedetti et al., 2015). Copepods used in the experiments were collected at the Lanveoc sampling site (48°18.00 N, 4°27.360 W) during cruises on-board the oceanographic ship "Albert Lucas" (INSU-CNRS-UBO) from January to April in years 2017 and 2018. Zooplankton were collected with a WP2 plankton net (200 µm mesh size) fitted with a 2 L filtering cod-end during horizontal net tows (speed < 1 m s^{-1} for <10 min) at 3 m depth. After each plankton haul, zooplankton samples were immediately diluted in 30 L of surface seawater, stored in the dark in a cool box, and brought back within few hours to the laboratory. To initiate the rearing phase, a ratio of 1 male per 5 females was assured with at least 100 (for *E. acutifrons*) to 250 (for calanoid copepods) adult females of each species individually sorted under a dissecting microscope. The copepods were placed in polycarbonate beakers of varying volume (from 7 to 20 L according to species size) containing 1 µm FSW. During at least 1 week of acclimation inside the culture room, copepods were kept at 18°C, at 33 salinity, and under 12:12 h day:night photoperiod for about up to 1 month. They were daily fed in excess with a mixture of algae continuously cultured (*Rhodomonas salina*, *Thalassiosira weissflogii*, *Tisochrysis lutea*, and *Tetraselmis suecica*, grown under the same condition as for *S. marinoi* and *C. neogracile*) at concentration exceeding

FIGURE 1 | Experimental design. **(Left)** Copepod grazing experiments on free diatom cells (Experiments 1–3). **(Right)** Copepod grazing experiments on diatom aggregates (Experiments 4–8). Photo on the **right** corresponds to *in situ* floating *Melosira* sp. aggregates between the ice packs, taken from the deck of the NGCC Amundsen at about 15 m distance.

10^3–10^4 cell mL^{-1} (Berggreen et al., 1988; Vincent et al., 2007), thus avoiding predation of calanoid copepods on younger stages (Bonnet et al., 2004; Boersma et al., 2014). Seawater was renewed every other day by adding 10–20% volume of 1 μm FSW and air was supplied *via* small bubbles in each rearing tank. Twenty-four hours prior to the beginning of the experiment, 30 (*C. helgolandicus*) to 100 (*E. acutifrons*) cultured copepods were isolated in 1 L beakers containing 0.2 μm FSW without food. This starving phase allowed gut evacuation and maximized feeding during incubation.

Wild *Calanus hyperboreus* (6.3 mm total length) were collected during the GreenEdge expedition on-board the NGCC Amundsen in July 2016. *C. hyperboreus* displays an omnivorous suspensive feeding behavior (Conover, 1966; Huntley, 1981; Greene, 1988; Darnis et al., 2008, 2012). Collection of zooplankton organisms *via* plankton nets resulted in retrieving high amounts of dead or injured individuals. The exact cause of this mortality could not be inferred and to undertake the grazing experiment, copepods were collected from 24 Niskin bottles (10 L) deployed over the 0–300 m depth at station 615 (70°29.926 N, 59°31.504 W). 240 L of seawater from the Niskin bottles was sieved over a 200 μm mesh sieve partially immersed in seawater to avoid individual stress. Only copepods of the *C. hyperboreus* species were collected. Immediately after sieving, copepods were isolated *via* pipetting in 1 L of 0.7 μm FSW and left for 24 h in the dark to limit stress and allow gut evacuation. On the day of the experiment, only the most active specimens

(N = 18) were collected using a sieve and added to the 4 L rolling tank containing the large *Melosira* sp. aggregate (Experiment 8).

Grazing Experiments

A set of eight laboratory experiments were carried out and allowed to integrate variable predator to prey size ratios, the latter ranging in size and type from small isolated diatom cell [6–10 μm equivalent spherical diameter (ESD)] up to few centimeters aggregates (**Tables 1**, **2**). For three out of the eight experiments carried out at laboratory (**Table 1**, Experiments 1–3), isolated diatom cells at exponential growth state were provided as food source at concentration higher than bloom density in the area (2.3–5.3 × 10^5 cell mL^{-1}), i.e., maximum cell concentrations of 10^4 cell mL^{-1} are generally recorded during bloom for *Chaetoceros* sp. and *Skeletonema* sp. (Soudant and Belin, 2018). This high diatom cell concentration was set on purpose to induce diatom collision and provided high likelihood to form aggregates during the course of the incubation. Aggregation of *S. marinoi* was indeed shown to take >40 h at cell density <10^5 cell mL^{-1} (Grossart et al., 2006). This high cell concentration was also chosen considering that even though copepod grazing could induce a large decrease in cell density (e.g., up to 50% of the initial stocks over the incubation at food density matching bloom), cell concentration would still remain close enough in controls compare to copepod tanks. The only differences in parameters promoting aggregation between the two tanks being related to copepod presence (i.e., swimming and grazing and possible

TABLE 1 | Initial conditions in incubations using freely suspended diatoms as prey (Experiments 1–3).

Experiment	Diatom species	Copepod species	Number of replicates	Copepod abundance (ind L^{-1})	Cell concentration (10^5 cell mL^{-1})	POC (μmol C L^{-1})	PON (μmol N L^{-1})	bSiO$_2$ (μmol Si L^{-1})	TEP (mg X$_{eq}$ L^{-1})	C:N (mol:mol)	Si:C (mol:mol)
1	S. marinoi	E. acutifrons	3	28.2 ± 0.0	5.3 ± 0.8	710 ± 124	45 ± 1	81 ± 2	5.2 ± 0.6	16 ± 3	0.11 ± 0.02
		C.helgolandicus	3	10.9 ± 0.6							
2	S. marinoi	E. acutifrons	3	33.9 ± 1.8	2.4 ± 0.2	414 ± 87	35 ± 0	74 ± 0	4.4 ± 1.7	12 ± 2	0.18 ± 0.04
3	C. neogracile	E. acutifrons	3	35.3 ± 0.0	2.3 ± 0.2	253 ± 11	30 ± 1	70 ± 1	3.5 ± 0.1	9 ± 0	0.28 ± 0.02
		A. clausi	3	14.9 ± 2.3							

Results are means ± SE.

change in mucus production, Malej and Harris, 1993). In the remaining four experiments (**Table 2**, Experiments 4–7), diatom aggregates were used as exclusive prey type. The incubation was initiated using 10–20 aggregates per roller tank (Guidi et al., 2008). Since the initial aggregate abundance varied during the first hours of the experiment as aggregation/disaggregation processes occurred before reaching an "equilibrium," the latter was chosen as the time set for estimating copepod effects (T$_0$). "Copepod tanks" received a known number of reared copepods as detailed in **Tables 1, 2**. In order to obtain a significant grazing signal, copepod abundance in rolling tanks was set high, i.e., being 2–4 times higher for calanoids and 10 times higher for *E. acutifrons* than those commonly measured *in situ* during the decline of phytoplankton blooms in the North Atlantic Ocean (typically 4 ind L^{-1} for calanoid copepods such as *T. longicornis*, *A. clausi*, and *C. helgolandicus* and 0.2 ind L^{-1} for harpacticoida (Schultes et al., 2013). However such high copepod abundances are totally congruent with those recorded over a 3-year survey in the eutrophic system of Long Island (Capriulo et al., 2002) with 30–50 ind L^{-1} for *T. longicornis* and >35 ind L^{-1} for *Acartia hudsonica*. These chosen abundance remained also highly comparable to values used in most experimental studies ranging from 8 to >15 ind L^{-1} (Sautour and Castel, 1993; Vincent and Hartmann, 2001; Sarthou et al., 2008). For all experiments, dead and injured individuals were discarded and living ones were individually pipetted to 1 L rolling tanks containing prey assemblages. Rolling tanks were then filled to the rim with FSW, avoiding air bubbles introduction and placed on the rolling table at 3 rpm. Tank rotation allowed prey homogenization and mimicked continuous settling of aggregates in the water column. Incubation was carried out at 18°C under natural photoperiod regime. Preliminary experiments permitted to set optimal incubation duration between 24 and 48 h (T$_f$ end of incubation) so as to measure adequate growth and grazing rates and limit bottle effects (Roman and Rublee, 1980).

During Experiment 8, the large *Melosira* sp. aggregate (26–34 mm) was incubated with wild copepods (*C. hyperboreus*) by adding 18 living individuals to a 4-L roller tank. The grazing experiment was undertaken at 4°C. *Melosira* sp. aggregates were shown to have strong negative buoyancy under light regime due to bubble formation induced by photosynthesis (Fernández-Méndez et al., 2014). Therefore, to keep aggregates suspended in the rolling tank during the experiment, the incubation with *C. hyperboreus* was undertaken in the dark and during 72 h to follow the temporal dynamic of the fragmentation and potential changes in copepod behavior.

Aggregates Enumeration, Size, and Sinking Velocity

Aggregate morphological characteristics were measured at T$_0$ and T$_f$ in rolling tanks before aggregate sampling. Image analyses were based on pictures and videos taken using a digital camera (Canon EOS 600D). Video recordings allowed to avoid aggregate manipulation and bias due to sampling. Aggregates were enumerated in each tank using image of the whole tank. Diameter (*d*, mm) and height (*h*, mm) of each aggregate (with *d* > *h*) were

Experiment	Diatom species	Copepod species	Number of replicates	Copepod abundance (ind L^{-1})	POC (μmol C L^{-1})	PON (μmol N L^{-1})	bSiO$_2$ (μmol Si L^{-1})	C:N (mol:mol)	Si:C (mol:mol)
4	C. neogracile	Control	4	–	64 ± 2	8.5 ± 0.2	2.6 ± 0.1	7.6 ± 0.2	0.04 ± 0.00
		E. acutifrons	4	34.3 ± 1.5					
5	C. neogracile	Control	4	–	na	na	na	na	na
		A. Clausi	4	16.6 ± 1.0					
6	S. marinoi	Control	4	–	128 ± 7	18 ± 1	13 ± 1	7 ± 0	0.10 ± 0.01
		T. longicornis	5	12.4 ± 2.0					
7	S. marinoi	Control	3	–	32 ± 2	2.8 ± 0.1	1.7 ± 0.1	11.5 ± 0.4	0.05 ± 0.01
		E. acutifrons	3	33.9 ± 1.8					
		C. helgolandicus	3	11.3 ± 0.6					
8	Melosira sp.	Control	2	–	33 ± 0	2.0 ± 0.1	2.8 ± 0.4	16.5 ± 0.6	0.08 ± 0.01
		C. hyperboreus	1	4.5					

Results are means ± SE; na stands for data not available.

derived from the pictures and estimated using an image system analysis software (Inkscape®) calibrated with the rolling tank characteristics (e.g., front diameter, back diameter, and width), measurement precision was 0.3 mm. A minimum of six images was used for each tank, all aggregates were individually measured on each picture unless aggregate concentration was >20 agg L^{-1}. In this case a minimum of 20 aggregates were analyzed in each picture (aggregate volume and ESD computations are presented in **Table 3**).

Aggregate sinking velocities (U_{agg}, m d^{-1}) were measured directly in the tank, using the method of Ploug et al. (2010). Sinking velocities of all aggregates were directly measured in the rolling tanks having aggregate concentrations <20 agg L^{-1}. In the tank where aggregate concentrations were higher, a minimum of 20 sinking velocities were independently measured. At steady state, aggregates follow a circular trajectory. For each aggregate, the rotation center of the aggregate was located using small video recordings and the software Inkscape®. Sinking velocities were deduced from the rotation of the tank and from the distance between the rotation center of the aggregate and the center of the tank, using Eq. 1.

$$U_{agg} = \frac{X_a}{T} \times 2\pi \quad (1)$$

where T is the tank rotation period (in d), and X_a the distance between the rotation center of the aggregate and the center of the tank (in m). As such, the error linked to sinking velocity computations is directly related to the minimum X_a measurable (0.3 mm) using image analysis, and the associated uncertainty is 0.7 m d^{-1}. Diatom aggregates are fractal particles, their sinking velocities increase with size according to a power law curve defined in Eq. 2 (Alldredge and Gotschalk, 1988; Iversen et al., 2010). The relation between sinking velocity (U_{agg}) and aggregate size (ESD) was computed for S. marinoi and C. neogracile aggregates, using a non-linear relation function nls() function; R software® (R Core Team, 2017).

$$U_{agg} = A(\text{ESD})^B \quad (2)$$

where A and B are the unidimensional parameters of the regression.

Final Sampling (T$_f$)

Aggregates were carefully removed from the rolling tank using a large aperture plastic pipette (10 mL) and isolated inside 50 mL falcon tubes containing FSW (one to four tubes were used depending on the amount of material). After being homogenized by vigorous shaking, subsamples were taken for chemical analyses. Once aggregates were removed, copepods were carefully retrieved from each rolling tank by sieving seawater through an immersed 200 µm mesh sieve. For Experiments 1–3 and 8, copepods were sorted and preserved in formalin solution (4% final concentration) for stage analyses and size estimations (length and width of the prosome and urosome). For Experiments 4–7, copepods were placed in 2 mL cryotubes (one per tank), flash frozen in liquid nitrogen in order to estimate aggregate ingestion via the gut content fluorescence method of Mackas and Bohrer (1976). Size measurements were made concurrently from 75 A. clausi, 79 C. helgolandicus, 100 T. longicornis, and 173 E. acutifrons, randomly sieved from the copepod culture over a 200 µm mesh sieve and preserved in formalin. Copepod size measurements were performed under a dissecting microscope and measurement precision was 10 µm.

Calanus helgolandicus fecal pellets from Experiments 1 (free cells) and 7 (aggregate) were recovered after the 24 h incubation by filtering the remaining seawater of each rolling tank onto a 40 µm mesh sieve. Fecal pellets retained on the mesh sieve were resuspended in FSW in a plankton counting chamber (Dolfuss cuvette, 6 mL volume), pipetted, and pooled into a 50 mL falcon tubes for size measurements and counting (see below).

Chemical Analyses
Biogenic Silica (bSiO$_2$)
Ten milliliters of the free cells or aggregate suspension were filtered through 0.4 µm polycarbonate filters (Millipore). For fecal pellet measurements, 100–200 fecal pellets of

TABLE 3 | Equations used to calculate volume (μm^3 and mm^3) and equivalent spherical diameter (ESD; μm and mm) for aggregates, fecal pellets, and copepods.

Description	Shape	Equation	Parameters	References
Aggregate volume (V_{agg}, μm^3)	Prolate spheroid shape	$V_{agg} = \frac{\pi}{6} \times d^2 \times h$	d = Aggregate diameter (μm) h = Aggregate height (μm)	Hillebrand et al., 1999
Fecal pellet volume (V_{PF}, μm^3)	Cylinder with two half spheres	$V_{PF} = \pi \times d^2 \times \left(\frac{L}{4} + \frac{d}{6}\right)$	L = Fecal pellet length (μm) d = Fecal pellet diameter (μm)	Hillebrand et al., 1999
Aggregate and fecal pellet equivalent spherical diameter (ESD, μm)		$ESD = \sqrt[3]{\frac{6 \times V}{\pi}}$		Hillebrand et al., 1999
T. longicornis volume (V_{cop}, μm^3)	Prolate spheroid shape (total volume)	$V_{cop} = \frac{4}{3} \times \pi \eta^2 \times \left(\frac{a}{2}\right)^3$	a = Prosome length (μm) η = Aspect ratio derived	Conway, 2006; Jiang and Kiørboe, 2011b
A. clausi, *C. helgolandicus*, and *C. hyperboreus* volume (V_{cop}, μm^3)	Ellipsoid shape (Prosome)	$V_p = \frac{\pi}{6} \times a \times b \times c$	a = Prosome length (μm) b = Prosome width (μm) c = Prosome height (μm)	Hillebrand et al., 1999
	Cylindrical shape (Urosome)	$V_u = r^2 \times \pi \times l$	l = Urosome length (μm) r = Urosome diameter (μm)	Hillebrand et al., 1999
		$V_{cop} = V_p + V_u$		
E. acutifrons volume (V_{cop}, μm^3)	Body shape-dependent conversion factors C	$V_{cop} = L \times W^2 \times C$	L = Total body length (μm) W = Total body width (μm) C = 485 for fusiform harpacticoid copepods	Warwick and Gee, 1984; Veit-Köhler, 2005
Copepod equivalent spherical diameter (ESD, μm)		$ESD_{cop} = \left(\frac{V_{cop}}{0.523}\right)^{1/3}$		Hansen et al., 1994

C. helgolandicus were directly placed on the filter. All filters were individually placed in petri dishes and dried at 55°C for 24 h. They were then kept at room temperature until $bSiO_2$ analysis following Moriceau et al. (2007). Briefly, filters were digested in 8 mL of sodium hydroxide (NaOH 0.2 M) during 4 h at 90°C under constant agitation. Digestion was stopped by cooling the solution to 4°C and neutralized with 2 mL of chloride acid (HCl 1 M). Digestates containing the dissolved silica (dSi) were analyzed using an AutoAnalyzer (Bran and Luebbe Technicon Autoanalyzer 0.1% precision).

Particulate Organic Carbon and Nitrogen

Ten milliliters of the free cell or aggregate suspensions were filtered through pre-combusted (4 h 450°C) glass fiber filters (Whatman GF/F). For fecal pellets measurements, 100–200 fecal pellets of *C. helgolandicus* were directly placed on the filter. All filters were then rinsed with 10 mL of FSW. The filters were placed inside aluminum foil, dried at 55°C for 24 h, and analyzed for elemental C and N using a Carlo Erba NA-1500 elemental analyzer (Aminot and Kérouel, 2004).

Transparent Exopolymeric Particles

Transparent exopolymeric particles were measured following the method of Passow and Alldredge (1995a) for Experiments 1–3. Sub-samples of 10 mL were pipetted from the cell suspension, and filtered onto 0.4 μm polycarbonate filters (Whatman) under low vacuum pressure (<60 mm Hg) in order to prevent TEP forcing through the filter pores. Filters were stained with 0.5 mL of Alcian blue solution for 2 s (0.02% in aqueous solution, 0.06% acetic acid, pH 2.5, filtered through 0.2 μm before use) and kept frozen (−20°C) until analysis. Filters were then soaked for 2 h

in 6 mL of 80% H_2SO_4 solution under constant agitation. The absorption of the obtained solution was measured at 787 nm (spectrophotometer prim'Light SECOMAM) in a 1 cm cuvette and was converted into mg of Gum Xanthan equivalent per liter (mg X_{eq} L^{-1}) using a calibration curve valid for our working solution of Alcian blue and made onto 0.2 μm polycarbonate filters. TEP concentrations were expressed in g X_{eq} L^{-1} and ng X_{eq} $cell^{-1}$, the latter taking into account the growth of the cells during the incubation. TEP production (ng X_{eq} $cell^{-1}$ d^{-1}) was calculated from the difference between TEP concentrations over the course of the incubation normalized by cell concentration at T_{init} and T_f.

Copepod ESD Computation

Copepod ESD was computed for each species from copepod volumes using shapes and equations from the literature (**Table 3**).

Specific Growth Rate and Grazing Parameters

Phytoplankton growth rates (k, d^{-1}), copepod grazing rates (g, d^{-1}), clearance rates (F, mL ind^{-1} d^{-1}), and ingestion rates were calculated from cell counts in Experiments 1–3 according to Frost (1972). At the beginning (T_{init}) and the end of incubation (T_f), 5 mL sub-samples of seawater from each tank were pipetted and preserved in acid Lugol solution (2% final concentration). Phytoplankton cell concentration was estimated using a Malassez cell counting chamber. Depending on cell density in the roller tanks, 3–12 sub-samples were counted corresponding to the enumeration of 120–300 cells per sample. When cell concentrations at T_f

were not significantly different between controls and copepod tanks, grazing was considered under the detection limit (i.e., <dl in **Table 4**). Ingestion rates were converted to ng Chl a ind^{-1} d^{-1} using a literature-based mean value of 0.10 pg Chl a cell^{-1} for *S. marinoi* (Norici et al., 2011; Chandrasekaran et al., 2014; Orefice et al., 2016; Smerilli et al., 2019) and 0.35 pg Chl a cell^{-1} for *C. neogracile* (unpublished data from González-Fernández et al., 2019).

Copepod Gut Content

For gut content analyses (Experiments 4–7), copepods were individually sorted from freshly thawed samples under a cool light stereomicroscope. Individuals were rinsed with 0.2 µm FSW to eliminate phytoplankton cells and aggregates stuck to feeding appendages, and were then transferred into 4 mL acetone (90%). Individuals ($N = 6$–27 copepods per replicate) were grinded and chlorophyllian pigments (Chlorophyll a and pheopigments) were extracted in the dark at 4°C overnight. Fluorescence of the extract was measured before and after acidification with 10% HCl (Parsons et al., 1984) using a Fluorometer (Turner design). Copepod gut content (G_{cop}, ng Chl a$_{eq}$ ind^{-1}) was obtained by addition of Chlorophyll *a* and pheopigments concentrations and values were not corrected for pigment degradation on the recommendation of Durbin and Campbell (2007). Ingestion rates (ng Chl a$_{eq}$ ind^{-1} h^{-1}) were derived from gut content (G_{cop}) using Eq. 3:

$$I = 60 \times G_{cop} \times k \tag{3}$$

where k is the gut evacuation rate (min^{-1}), computed following the model of Dam and Peterson (1988) which accounts for the temperature of incubation.

Fecal Pellet Production, Size, and Sinking Velocities

Fecal pellets production (FP ind^{-1} d^{-1}) was estimated in experiments with *C. helgolandicus* (Experiments 1–7). Up to six sub-samples of the total fecal pellet suspension were counted. Each fecal pellet was measured (length and width in µm) with 10 µm precision (see **Table 3** for shape and volume computations).

Fecal pellet sinking velocities (U_{FP}, m d^{-1}) follow Stokes' law and were computed following Eq. 4 (Komar et al., 1981).

$$U_{FP} = 0.0790 \times \frac{1}{\mu} \times (\rho_{SW} - \rho_{PF}) \times g \times L^2 \left(\frac{L}{d}\right)^{-1.604} \tag{4}$$

where µ is the kinetic viscosity of seawater (0.0123 g cm^{-1} s^{-1}), ρ_{SW} and ρ_{PF} are the density of seawater (1.071 g cm^{-3} at 18°C) and of *C. helgolandicus* fecal pellets (1.26 g cm^{-3}; Cole et al., 2016), respectively, L and d the fecal pellet length (cm) and width (cm), respectively, and g is the acceleration due to gravity (981 cm s^{-2}).

Statistical Analyses

Results are expressed in mean ± standard error (SE), or ±cumulative error when manipulations or analysis involved error propagation (e.g., aggregates abundances, TEP production, Si:C ratios, and C:N ratios). Statistics were performed using Sigmaplot® 14.0 software. As data distribution matched the parametric assumption of normality (using Shapiro–Wilk test, $p < 0.05$), the effects of copepod grazing on the mean size, aggregate abundance, and stoichiometric ratios during the incubation were tested by one-way ANOVA. Tukey's *post hoc* tests were used to determine specific copepod influence on measured parameters. Covariance between ESD and sinking velocity was analyzed on logarithmic transformed data using an ANCOVA. Linear correlation between two variables was analyzed using Pearson correlation test under assumption of normality, and using Spearman rank correlation test when otherwise.

RESULTS

First Set of Experiments: Effects of Copepod Grazing/Swimming on Diatom Aggregation

Copepod Ingestion Rates

During the incubations, copepods actively grazed on *S. marinoi* (Experiments 1 and 2) but no grazing was measurable on *C. neogracile* (Experiment 3), i.e., phytoplankton growth exceeded grazing rates as evidenced by similar cell abundance

TABLE 4 | Final cell concentration (10^5 cell mL^{-1}) and copepod clearance (mL ind^{-1} d^{-1}) and ingestion rates (ng Chl a ind^{-1} d^{-1}) for Experiments 1–3.

Experiment	Diatom species	Copepod species	Final cell concentration (10^5 cell mL^{-1})	Clearance rate (mL ind^{-1} d^{-1})	Ingestion rate (ng Chl a ind^{-1} d^{-1})
1	*S. marinoi*	Control	5.8 ± 0.8	–	–
		E. acutifrons	5.9 ± 1.0	3 ± 3	157 ± 155
		C. helgolandicus	4.4 ± 0.3	24 ± 6	1159 ± 248
2	*S. marinoi*	Control	3.6 ± 0.1	–	–
		E. acutifrons	2.63 ± 0.03	9.6 ± 0.3	225 ± 6
3	*C. neogracile*	Control	2.8 ± 0.2	–	–
		E. acutifrons	3.0 ± 0.1	<dl	<dl
		A. clausi	3.07 ± 0.04	<dl	<dl

Results are means ± SE; <dl, under the detection limit.

in controls and copepod tanks at T_f (**Table 4**). *E. acutifrons* ingestion rates ranged from 157 ± 155 to 225 ± 6 ng Chl a ind^{-1} d^{-1} (**Table 4**). *C. helgolandicus* ingestion rates were five to eight times higher, reaching 1159 ± 248 ng Chl a ind^{-1} d^{-1} (**Table 4**). During the incubation with *S. marinoi*, *C. helgolandicus* egestion averaged 64 ± 55 fecal pellets ind^{-1} d^{-1} (Experiment 1). Their average ESD was 173 ± 24 μm, with a carbon content of 30 ± 7 nmol C PF^{-1} and a sinking velocity of 122 ± 32 m d^{-1}. The majority of fecal pellets recovered at the end of the incubation were intact.

Aggregation of Free Diatom Cells

Sizes and sinking velocities of the *S. marinoi* aggregates formed in the presence of *E. acutifrons* and *C. helgolandicus* were not significantly different from the controls with respective mean values of 1.6 ± 0.0 mm ESD and 230 ± 1 m d^{-1} (**Table 5** and **Figure 2A**). At lower cell density, *S. marinoi* formed less but bigger aggregates than during Experiment 1, with a mean ESD of 3.1 ± 0.6 mm (**Table 5** and **Figure 2C**) and an average sinking velocity of 320 ± 10 m d^{-1} (**Table 5**). However, mean aggregate abundance was significantly higher (*p*-value < 0.05) in Experiment 1 in the presence of *E. acutifrons* (288 ± 80 agg L^{-1}) compared to controls (145 ± 25 agg L^{-1}) and *C. helgolandicus* (113 ± 35 agg L^{-1}) (**Table 5** and **Figure 2B**). At lower initial cell concentration (Experiment 2), aggregate abundance was also slightly higher (but not significantly) in *E. acutifrons* tanks, with a mean of 60 ± 9 agg L^{-1} compared to 46 ± 9 agg L^{-1} in controls (**Table 5** and **Figure 2D**). A non-significant but systematic increase in the TEP concentration or production by *S. marinoi* was measured in the presence of *E. acutifrons* and *C. helgolandicus* (**Table 5**). Concerning Experiment 3 with *C. neogracile*, aggregates were formed in two out of the six copepod tanks (**Table 5**). In the rolling tanks containing *A. clausi* (Experiment 3), TEP production was significantly higher than in controls (4 ± 2 versus 10 ± 3 pg X_{eq} cell^{-1} d^{-1}, $p = 0.045$). *C. neogracile* formed larger aggregates than *S. marinoi* with average ESD of 4.5 ± 0.5 and 4.3 ± 1.5 mm in the presence of *E. acutifrons* and *A. clausi*, respectively. In this experiment, *C. neogracile* aggregates were too numerous and had too low contrast in pictures and videos to measure their sinking velocity, probably due to their low cell content. Indeed, the percentage of aggregated cells was only $0.3 \pm 0.3\%$ (**Table 5**).
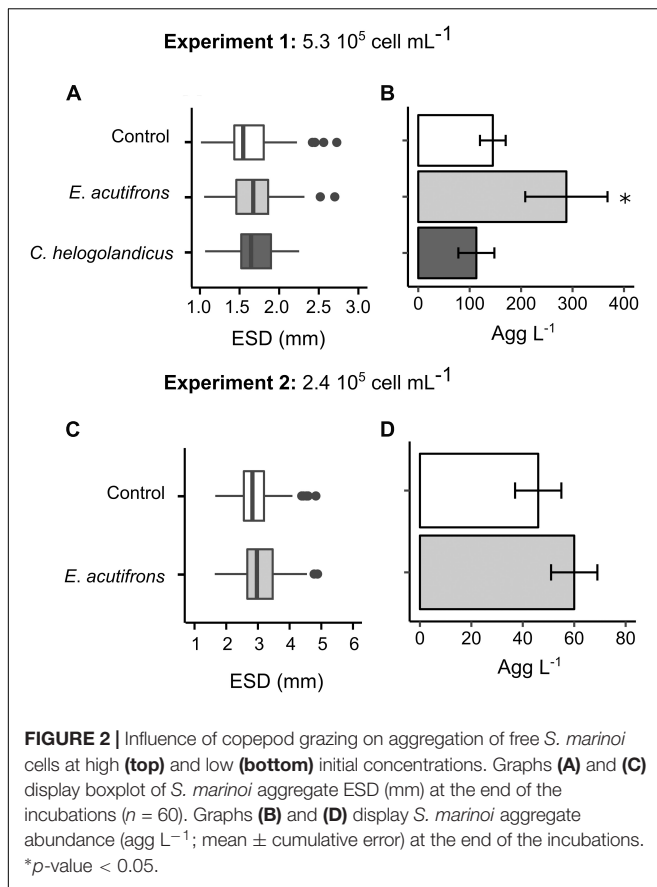
Elemental Cell Composition

Si:C ratios of *S. marinoi* significantly increased from 0.14 ± 0.04 to 0.21 ± 0.04 ($p = 0.018$) in the presence of *E. acutifrons* (Experiment 1), whereas *C. helgolandicus* grazing did not influence Si:C nor C:N ratios (Experiment 1). In general *S. marinoi* C:N ratios decreased similarly in all rolling tanks ($p < 0.05$), except for Experiment 1 where *E. acutifrons* grazing led to a stronger decrease of *S. marinoi* C:N ratio. *C. neogracile* elementary ratios were not modified during incubation in the presence or absence of copepods (controls), as shown by the marked stability in mean values of Si:C and C:N ratios (**Table 5**).

TABLE 5 | Final conditions in incubations (Experiments 1–3) using free diatom cells as prey.

Experiment	Diatom species	Copepod species	Aggregate abundance (agg L^{-1})	ESD (mm)	Sinking velocity (m d^{-1})	Aggregated cells (% of total cells)	Final TEP concentration (mg X_{eq} L^{-1})	TEP production (pg X_{eq} cell^{-1} d^{-1})	Final C:N (mol:mol)	Final Si:C (mol:mol)
1	*S. marinoi*	Control	145 ± 25	1.6 ± 0.1	230 ± 65	29 ± 12	5.9 ± 0.8	1 ± 2	10.2 ± 2.4	0.14 ± 0.04
		E. acutifrons	$288 \pm 80^*$	1.6 ± 0.0	228 ± 54	39 ± 6	6.7 ± 0.6	3 ± 1	6.4 ± 0.6	$0.21 \pm 0.04^*$
		C. helgolandicus	113 ± 35	1.6 ± 0.1	232 ± 64	29	6.4 ± 0.9	2 ± 2	8.0 ± 2.5	0.16 ± 0.06
2	*S. marinoi*	Control	46 ± 9	3.0 ± 0.3	310 ± 16	32 ± 10	5.1 ± 0.5	2 ± 2	8.6 ± 0.3	0.21 ± 0.01
		E. acutifrons	60 ± 9	3.1 ± 0.2	330 ± 12	13 ± 2	6.0 ± 0.5	7 ± 2	7.7 ± 0.4	0.19 ± 0.02
3	*C. neogracile*	Control	No agg.	No agg.	No agg.	0	4.4 ± 0.7	4 ± 2	7.8 ± 0.7	0.26 ± 0.05
		E. acutifrons	47 ± 47	4.5 ± 0.5	<dl	23 ± 23	5.7 ± 1.3	9 ± 5	10.1 ± 1.2	0.21 ± 0.03
		A. clausi	2 ± 2	4.3 ± 1.5	<dl	0.3 ± 0.3	$6.2 \pm 0.9^*$	$10 \pm 3^*$	7.5 ± 0.8	0.26 ± 0.03

*Results are means ± SE, except for aggregate abundance, TEP production, and C:N and Si:C ratios where means ± cumulative error are indicated. *p-value < 0.05; <dl, under the detection limit; No agg., no aggregation.*

FIGURE 2 | Influence of copepod grazing on aggregation of free *S. marinoi* cells at high **(top)** and low **(bottom)** initial concentrations. Graphs **(A)** and **(C)** display boxplot of *S. marinoi* aggregate ESD (mm) at the end of the incubations (n = 60). Graphs **(B)** and **(D)** display *S. marinoi* aggregate abundance (agg L^{-1}; mean ± cumulative error) at the end of the incubations. *p-value < 0.05.

TABLE 6 | Copepod gut contents (ng Chl a$_{eq}$ ind^{-1}) and ingestion rates (ng Chl a$_{eq}$ ind^{-1} d^{-1}) while grazing on aggregates (Experiments 4–7).

Experiment	Diatom species	Copepod species	Gut content (ng Chl a$_{eq}$ ind^{-1})	Ingestion rate (ng Chl a$_{eq}$ ind^{-1} d^{-1})
4	C. neogracile	E. acutifrons	0.08 ± 0.03	4 ± 1
5	C. neogracile	A. clausi	0.12 ± 0.04	6 ± 2
6	S. marinoi	T. longicornis	0.5 ± 0.3	23 ± 14
7	S. marinoi	E. acutifrons	0.05 ± 0.02	2.6 ± 0.9
		C. helgolandicus	0.3 ± 0.2	14 ± 9

Results are means ± SE.

Second Set of Experiments: Effects of Copepod Grazing/Swimming on Aggregate Dynamics

Copepod Grazing on *C. neogracile* Aggregates

Chaetoceros neogracile aggregates were grazed by both *E. acutifrons* and *A. clausi* as proven by copepod mean gut contents values reaching 0.08 ± 0.03 and 0.12 ± 0.04 ng Chl a$_{eq}$ ind^{-1} for *E. acutifrons* and *A. clausi*, respectively (**Table 6**). Derived ingestion rates ranged from 4 ± 1 to 6 ± 2 ng Chl a$_{eq}$ ind^{-1} d^{-1} for *E. acutifrons* and *A. clausi*, respectively (**Table 6**).

C. neogracile Aggregate Distribution and Sinking Velocity

In Experiment 4, no significant changes in *C. neogracile* aggregate abundance, ESD, and sinking velocity were observed in the presence of *E. acutifrons* (**Table 7** and **Figures 3A,B**). During Experiment 5, re-aggregation was observed in all rolling tanks causing a shift in aggregate abundance (from 18 ± 6 to 3 ± 1 agg L^{-1} in controls and from 15 ± 3 to 1.7 ± 0.6 agg L^{-1} with *A. clausi*), size (from 1.8 ± 0.1 to 5 ± 1 mm in controls and from 1.9 ± 0.1 to 5 ± 1 mm with *A. clausi*), and sinking velocity (from 141 ± 27 to 439 ± 153 m d^{-1} in controls and from 145 ± 26 to 501 ± 106 m d^{-1} with *A. clausi*), between T$_0$ and T$_f$ (**Table 7** and **Figures 3C,D**). This pattern was similar in copepod

and control tanks suggesting that grazing by *A. clausi* had no influence on aggregation dynamics (**Table 7** and **Figures 3C,D**).

Elemental Composition of the *C. neogracile* Aggregates

Euterpina acutifrons grazing on *C. neogracile* aggregates did not influence the particulate organic matter elemental composition and mean values remained stable, with final C:N ratios of 7.9 ± 0.3, and final Si:C ratios of 0.04 ± 0.02 (**Table 7**). Due to technical problems, no data were available for Experiment 5.

Copepod Grazing on *S. marinoi* Aggregates

All copepods studied fed on *S. marinoi* aggregates (Experiments 6 and 7). This resulted in mean gut content values of 0.5 ± 0.3 ng Chl a$_{eq}$ ind^{-1} for *T. longicornis* and 0.3 ± 0.2 ng Chl a$_{eq}$ ind^{-1} for *C. helgolandicus*. The smallest copepod *E. acutifrons* exhibited the lowest values with an average of 0.05 ± 0.02 ng Chl a$_{eq}$ ind^{-1} (**Table 6**). Derived ingestion rates reached 23 ± 14 ng Chl a$_{eq}$ ind^{-1} d^{-1} for *T. longicornis*, 14 ± 9 ng Chl a$_{eq}$ ind^{-1} d^{-1} for *C. helgolandicus*, and 2.6 ± 0.9 ng Chl a$_{eq}$ ind^{-1} d^{-1} for *E. acutifrons* (**Table 6**).

Calanus helgolandicus fecal pellets collected were intact, and fecal pellet mean production rate was 25 ± 3 FP ind^{-1} d^{-1}, which is a twofold lower value than what was observed when grazing on free *S. marinoi* (Experiment 1). Fecal pellets produced were smaller when aggregates were the only prey, averaging 145 ± 25 µm in ESD. Corresponding carbon content (33 ± 7 nmol C PF^{-1}) and sinking velocity (97 ± 31 m d^{-1}) were also lower.

S. marinoi Aggregates Distribution and Sinking Velocity

The presence of *T. longicornis* induced a fragmentation of aggregates evidenced by a significant increase in aggregate abundance (from 3 ± 1 to 14 ± 8 agg L^{-1}; p = 0.039) and a significant decrease in their mean ESD (from 9 ± 3 to 4.1 ± 0.7 mm; p = 0.013). As a consequence, corresponding sinking velocities were twofold higher in controls at T$_f$ compared to copepod tanks (**Table 7** and **Figures 4A,B**). During Experiment 7, re-aggregation processes were observed in all incubations suggesting no influence of copepod presence (**Table 7** and **Figures 4C–E**).

TABLE 7 | Initial and final aggregate abundances (agg L^{-1}), ESD (mm), and associated sinking velocities (m d^{-1}) in incubations using aggregates as copepod prey (Experiments 4–8).

Experiment	Diatom species	Copepod species	Initial aggregate abundance (agg L^{-1})	Final aggregate abundance (agg L^{-1})	Initial ESD (mm)	Final ESD (mm)	Initial sinking velocity (m d^{-1})	Final sinking velocity (m d^{-1})	Final C:N (mol:mol)	Final Si:C (mol:mol)
4	C. neogracile	Control	3 ± 1	1.8 ± 0.9	7 ± 2	9 ± 2	265 ± 105	384 ± 78	7.9 ± 0.2	0.04 ± 0.02
		E. acutifrons	6 ± 1	4 ± 2	4.5 ± 0.4	10 ± 5	191 ± 28	423 ± 199	8 ± 0.2	0.04 ± 0.02
5	C. neogracile	Control	18 ± 6	3 ± 1	1.8 ± 0.1	5 ± 1	141 ± 27	439 ± 153	NA	NA
		A. clausi	15 ± 3	1.7 ± 0.6	1.9 ± 0.1	5 ± 1	145 ± 26	501 ± 106	NA	NA
6	S. marinoi	Control	3 ± 2	4 ± 3	13 ± 7	10 ± 4	967 ± 755	809 ± 378	6.8 ± 0.1	0.12 ± 0.05
		T. longicornis	3 ± 1	14 ± 8*	9 ± 3	4.1 ± 0.7*	840 ± 505	367 ± 70	6.8 ± 0.2	0.14 ± 0.08
7	S. marinoi	Control	7 ± 1	1.9 ± 0.6	2.00 ± 0.02	4 ± 1	401 ± 30	457 ± 179	7 ± 2	0.10 ± 0.06
		E. acutifrons	6 ± 2	2.4 ± 0.8	2.3 ± 0.1	4.2 ± 0.7	474 ± 7	482 ± 131	4 ± 2	0.2 ± 0.1
		C. helgolandicus	11 ± 4	1.4 ± 0.4	1.9 ± 0.1	4.5 ± 0.7	382 ± 15	498 ± 143	6 ± 1	0.18 ± 0.06
8	Melosira sp.	Control	0.25	0.3 ± 0 (at T 72 h)	26.75 ± 0.05	30 ± 4	1540 ± 70	1633 ± 422	11 ± 2	0.18 ± 0.03
		C. hyperboreus	0.25	13 ± 1 (at T 72 h)	34	10 ± 4 (at T 48 h)	1779	740 ± 351 (at T 48 h)	10 ± 1 (at T 72 h)	0.14 ± 0.03 (at T 72 h)

Results are means ± SE, except for C:N and Si:C ratios where means ± cumulative error are indicated. *p-value < 0.05.

Elemental Composition of S. marinoi Aggregates

We did not observed any significant variation of Si:C and C:N ratios over time and between tanks. Ratios remained stable reaching respective mean ratios of 0.13 ± 0.07 and 6.8 ± 0.2 for Si:C and C:N, respectively, in Experiment 6 and mean ratios of 0.14 ± 0.11 and 6 ± 3 for Si:C and C:N, respectively, in Experiment 7 (**Table 7**).

In situ Experiment: Effects of C. hyperboreus Grazing/Swimming on Melosira sp. Aggregate Characteristics and Elemental Composition

The Melosira sp. aggregates formed at T_{init} were stable in size and sinking rates over the 72 h incubation in controls (**Table 7**). By contrast, after 24 h incubation with C. hyperboreus the fragmentation of this large aggregate into seven smaller ones (1.75 agg L^{-1}) of 14.3 ± 7.0 mm ESD and associated mean sinking velocity of 1017 ± 257 m d^{-1} was evidenced. Fragmentation processes were ongoing over time and after 48 h resulted in an aggregate abundance of 4.8 agg L^{-1} (with respective ESD of 9.8 ± 2.7 mm and average sinking velocity of 740 ± 351 m d^{-1}, **Table 7** and **Figure 5**). After 72 h, incubation with copepods resulted in 50 ± 12 aggregates (12.5 ± 1.2 agg L^{-1}). Due to the huge amount of small particles and the low quality of the video recordings, size and sinking velocities measurements could not be done at 72 h.

While it was not possible to measure ingestion, analyses of videos showed active interactions between copepods and aggregates. Copepods were ripping aggregates or swimming through aggregates. We observed a switch in C. hyperboreus swimming behavior between T_0 and T_f. In fact, during the first hours of incubation while only one large aggregate was present, copepods were passively swept within the rolling tank rotation and only exhibited few jumps. After 48 h of incubation, copepods were more active and we observed several jumps, and changes in swimming trajectories to avoid collision with aggregates (**Figure 6** and **Supplementary Videos S2, S3**).

When C. hyperboreus were incubated during 72 h with Melosira sp. aggregates, we did not observe any changes in Si:C and C:N ratios, compared to the controls and mean values were 0.16 ± 0.02 and 11 ± 1, respectively (**Table 7**).

DISCUSSION

Methodological Considerations

The main purpose of this study was to investigate the influence of copepod grazing/swimming on aggregate formation and dynamics. Aggregate formation depends on coagulation processes regulated by particle stickiness and collision rate inside the tank, the latter being directly linked to particle concentration (Jackson, 1990, 2015; Riebesell, 1991). Our experimental set up allowed to study if copepod activity favored or prevented aggregate formation, independently from particle concentration variations due to grazing and swimming. Despite the high cell concentrations needed to promote aggregation in 24 h, grazing
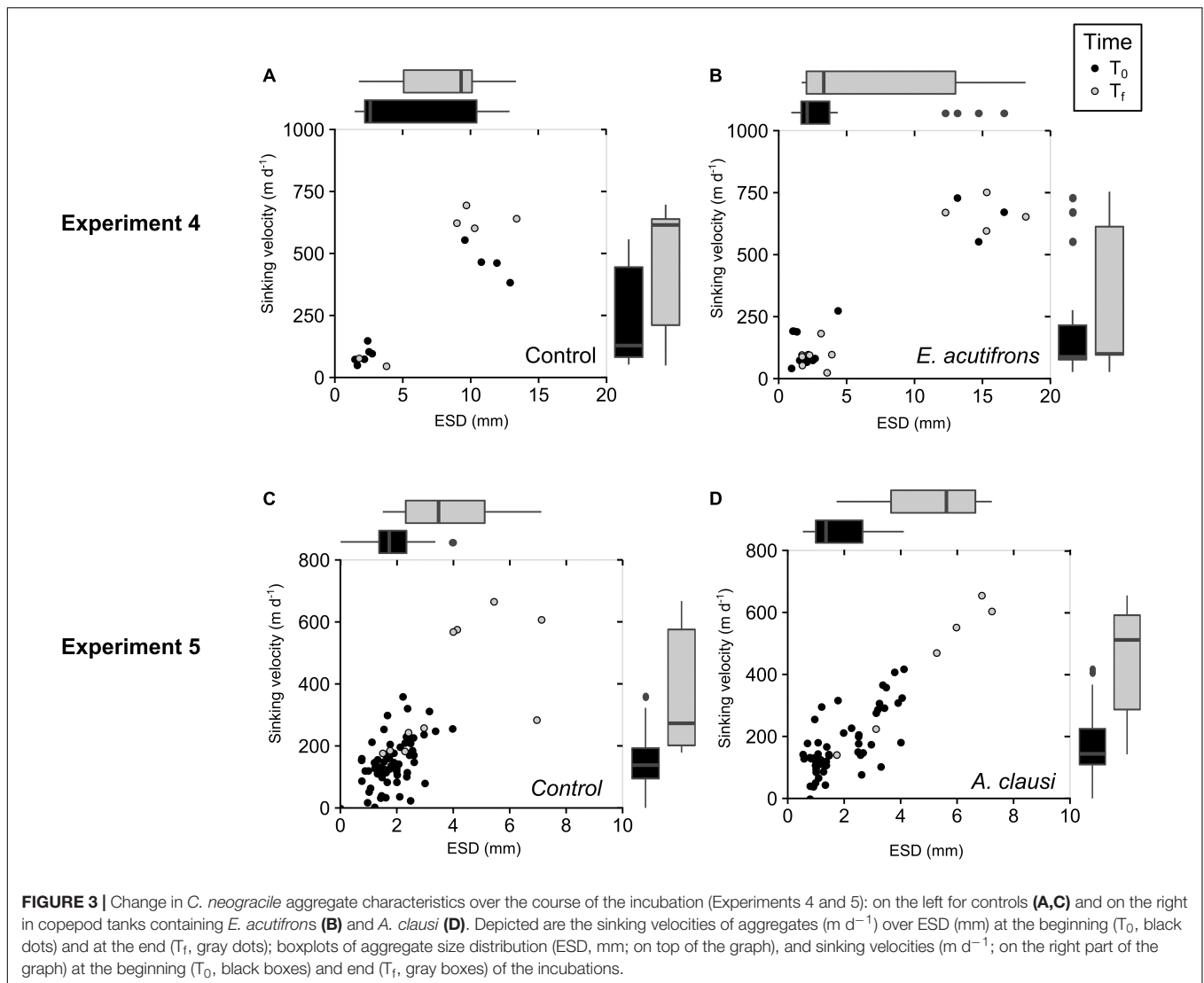
FIGURE 3 | Change in *C. neogracile* aggregate characteristics over the course of the incubation (Experiments 4 and 5): on the left for controls **(A,C)** and on the right in copepod tanks containing *E. acutifrons* **(B)** and *A. clausi* **(D)**. Depicted are the sinking velocities of aggregates (m d^{-1}) over ESD (mm) at the beginning (T$_0$, black dots) and at the end (T$_f$, gray dots); boxplots of aggregate size distribution (ESD, mm; on top of the graph), and sinking velocities (m d^{-1}; on the right part of the graph) at the beginning (T$_0$, black boxes) and end (T$_f$, gray boxes) of the incubations.

activity was still measurable in all experiments except Experiment 3. Clearance rates of 3–9.6 mL ind^{-1} d^{-1} for *E. acutifrons* and of 24 ± 6 mL ind^{-1} d^{-1} for *C. helgolandicus* were congruent with literature values for the same species, e.g., from 2.8 to 31 mL ind^{-1} d^{-1} for *E. acutifrons* (Sautour and Castel, 1993; de Melo Júnior et al., 2013), and from 36 to 126 mL ind^{-1} d^{-1} for *C. helgolandicus* (Fileman et al., 2007). The same holds for ingestion rates, our values for *E. acutifrons* are highly comparable with values recorded during laboratory experiments (157–225 ng Chl a ind^{-1} d^{-1}, this study vs. 360–408 ng Chl a ind^{-1} d^{-1} in Sautour and Castel, 1993). By contrast, *C. helgolandicus* exhibited ingestion rates twofold higher (1159 ± 248 ng Chl a ind^{-1} d^{-1}) than the value found in Irigoien et al. (2000) (600 ng Chl a ind^{-1} d^{-1}) and rates commonly range between 30 and 300 ng Chl a ind^{-1} d^{-1}, depending on food concentration (Mauchline, 1998; Fileman et al., 2007). In our study, this discrepancy could be explained by the combined effects of high prey concentration, the absence of stress due to predation, and the 24 h starvation phase prior to the beginning of the experiment, all these factors

being acknowledged to maximize ingestion (Bollens and Frost, 1989a,b, 1991; Bollens and Stearns, 1992; Mauchline, 1998).

In the second set of experiments (Experiments 4–7), it was impossible to use the Frost (1972) method to compute grazing rates. Firstly because aggregates are complex cell assemblages preventing the measurement of the exponential phytoplankton growth. Secondly, the high heterogeneity of aggregates does not allow to rely precisely on the same initial Chl a concentration in each tank, and may thus introduce biases in rate computations. As an alternative, ingestion rates were estimated from the gut fluorescent content method (Mackas and Bohrer, 1976) which is often performed at laboratory or *in situ* to estimate zooplankton herbivory. It constitutes a fast and easy method to set up that could be carried out on a variety of planktonic (copepods, salps, and krill; Pakhomov et al., 1996; Perissinotto and Pakhomov, 1998; Lópes et al., 2007), pelagic (herring larvae, Denis et al., 2018), and benthic organisms (Díaz et al., 2012; Gaonkar and Anil, 2012). Although potential issues exist regarding gut pigments destruction (Conover et al., 1986;
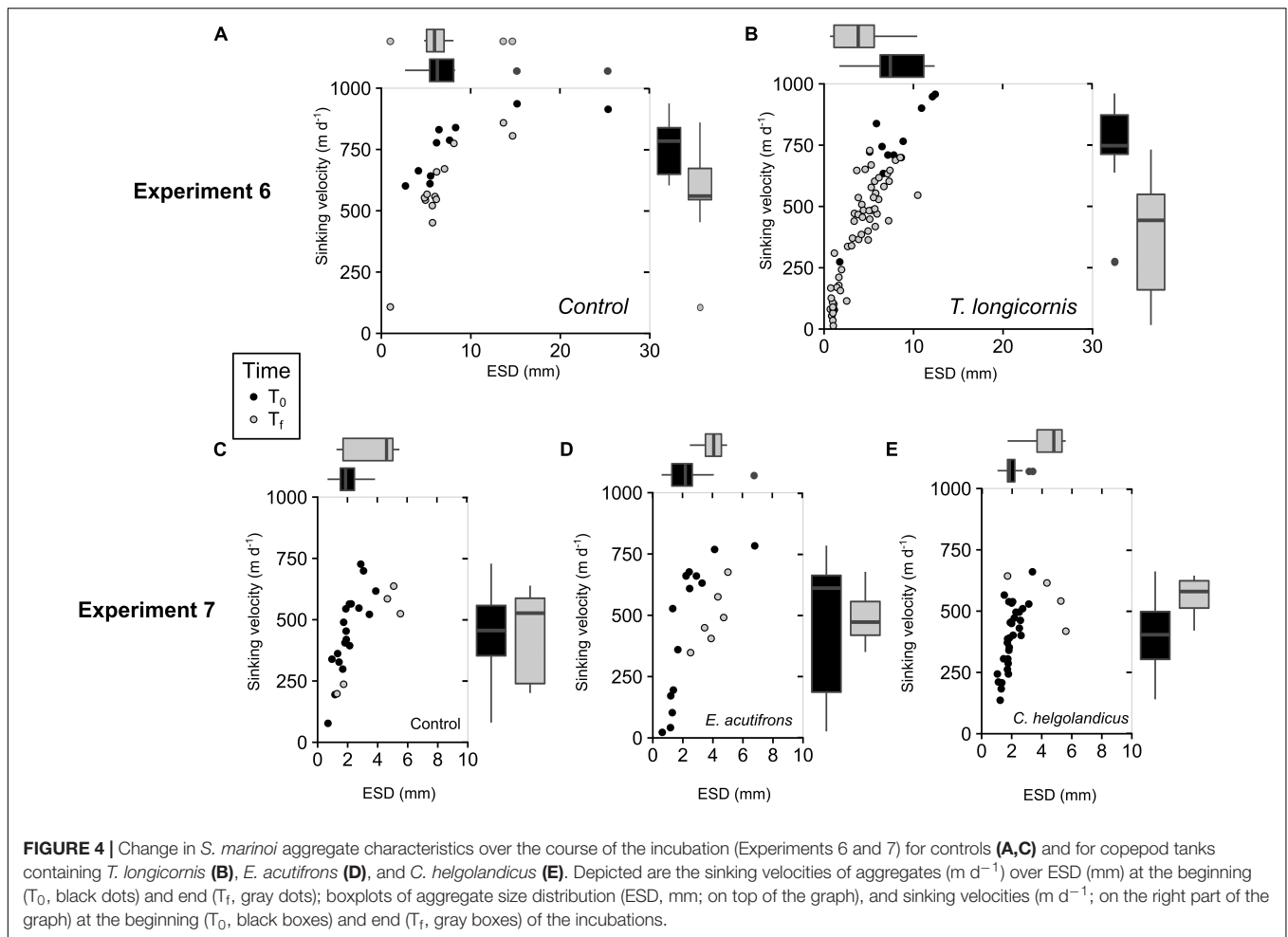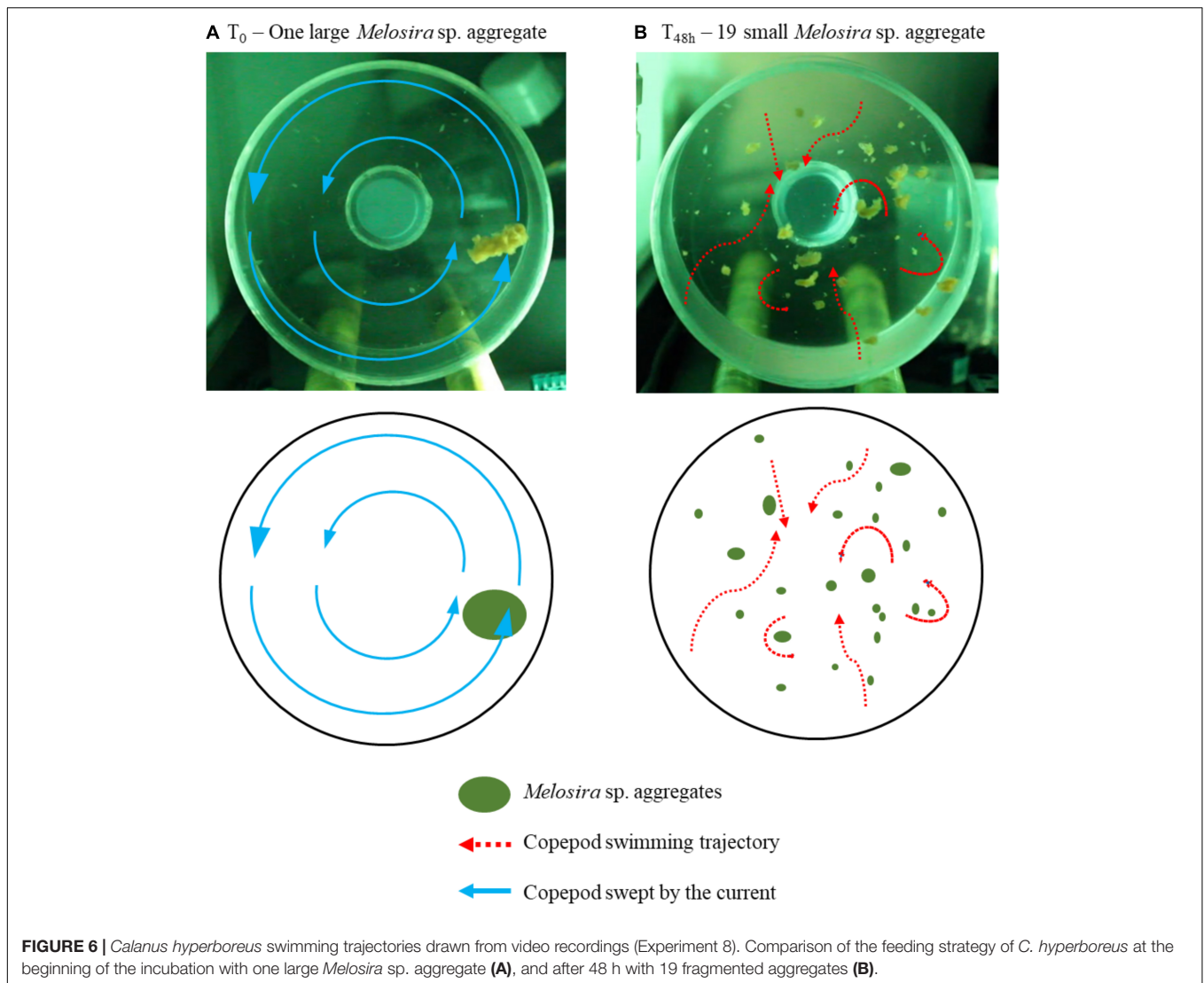
FIGURE 4 | Change in *S. marinoi* aggregate characteristics over the course of the incubation (Experiments 6 and 7) for controls **(A,C)** and for copepod tanks containing *T. longicornis* **(B)**, *E. acutifrons* **(D)**, and *C. helgolandicus* **(E)**. Depicted are the sinking velocities of aggregates (m d^{-1}) over ESD (mm) at the beginning (T_0, black dots) and end (T_f, gray dots); boxplots of aggregate size distribution (ESD, mm; on top of the graph), and sinking velocities (m d^{-1}; on the right part of the graph) at the beginning (T_0, black boxes) and end (T_f, gray boxes) of the incubations.
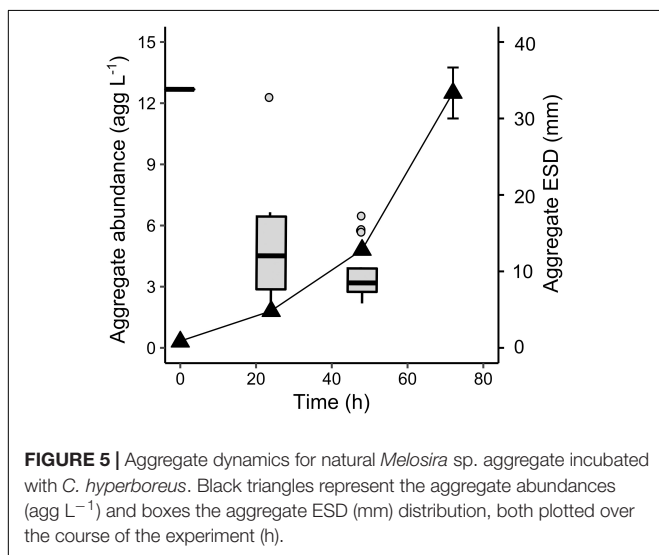
FIGURE 5 | Aggregate dynamics for natural *Melosira* sp. aggregate incubated with *C. hyperboreus*. Black triangles represent the aggregate abundances (agg L^{-1}) and boxes the aggregate ESD (mm) distribution, both plotted over the course of the experiment (h).
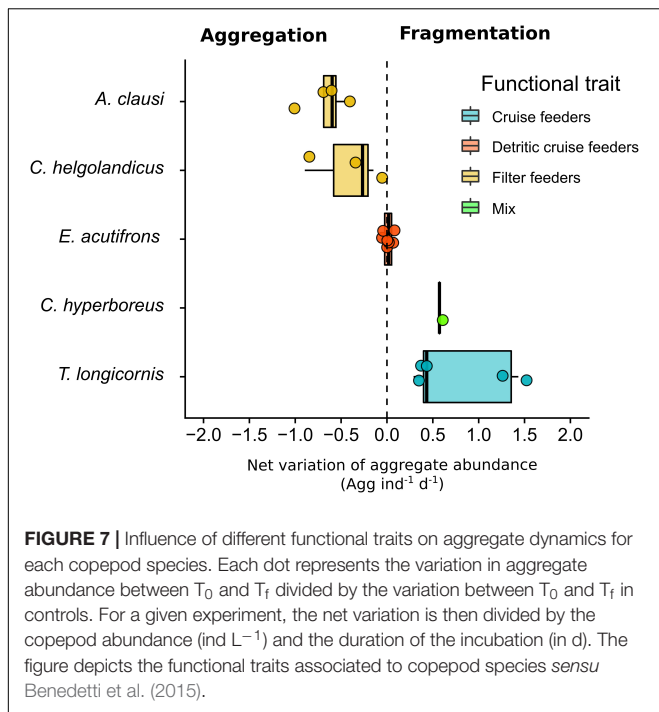
Durbin and Campbell, 2007) and gut evacuation rate estimates (Perissinotto and Pakhomov, 1996), the method appeared well suited to quantify aggregate ingestion by copepods, using total chlorophyllian pigments as a proxy of prey biomass. The ingestion rates obtained *via* gut content are, however, not directly comparable to those estimated from cell decrease (e.g., Frost, 1972) and rather correspond to a snapshot of the amount of aggregates ingested at the time of sampling. In any case, our results highlighting significant ingestion of most copepod species while offered aggregate as prey, revealed copepod ability to deal with larger and more complex preys (i.e., containing a mix of cell and mucus assemblage) such as whole or fragmented aggregates as shown by Iversen and Poulsen (2007), when copepods were offered fecal pellets as food. If copepod preferences for fragmented aggregates could not be inferred from our study, direct feeding on large aggregates was observed for *E. acutifrons* and *C. hyperboreus*, and individuals seemed to hang on aggregates while feeding (**Supplementary Video S1** for *E. acutifrons*).

First Set of Experiments: Copepod Grazing/Swimming Effects on Diatom Aggregation

Different processes could explain how copepod presence have modified cell aggregation dynamic in our study.

FIGURE 6 | *Calanus hyperboreus* swimming trajectories drawn from video recordings (Experiment 8). Comparison of the feeding strategy of *C. hyperboreus* at the beginning of the incubation with one large *Melosira* sp. aggregate **(A)**, and after 48 h with 19 fragmented aggregates **(B)**.

Cell stickiness may be enhanced when TEP production is boosted. Exudation of organic compounds and polymers by zooplankton is well known (Alldredge and Silver, 1988; Schuster and Herndl, 1995). In general, copepod cues may also induce physiological responses in marine phytoplankton. For instance, copepodamides are compounds that may induce defensive traits such as increase in toxin production by dinoflagellates (Selander et al., 2011, 2015), change in *S. marinoi* chain size (Bergkvist et al., 2012, 2018; Amato et al., 2018; Grebner et al., 2018) and increase the silica content of *T. weissflogii* (Pondaven et al., 2007). In line with the study of Malej and Harris (1993) who measured an inhibition of copepod feeding rate due to high molecular weight polysaccharides produced by phytoplankton, we hypothesized in our experiments that copepod activities may promote mucus production as observed for nutrient limitation stress (Engel, 2000; Passow, 2002). Indeed TEP production in Experiment 3 was higher when *A. clausi* grazed on *C. neogracile* and slightly higher (though not significantly) in the presence of *E. acutifrons* (Experiment 1) than in controls. However, while more

aggregates were produced with *E. acutifrons*, we did not observe an increase in aggregate formation with *A. clausi*. Conversely to the general postulate stating that aggregation is positively correlated to TEP concentrations, in our study, higher TEP production did not always result in higher aggregation rate, at least during the 24 h of incubation. Moreover, no significant correlation was found between TEP production or concentration and aggregate abundance or size. While TEP are important to trigger aggregation, TEP concentrations and production alone are not sufficient to explain our aggregation patterns.

The collision rates may be modified by two parameters: micro-turbulences created when copepods swim around and particle abundances associated to differential sinking due to egestion of fast sinking fecal pellets and manipulation of TEP by copepods. To aggregate, the particles must collide and then stick together. However, if the collision is too violent (high energy dissipation rates see Alldredge et al., 1990), no coagulation follows and disaggregation processes may even occur (Alldredge et al., 1990). In rolling tanks without copepods, collision is promoted through

FIGURE 7 | Influence of different functional traits on aggregate dynamics for each copepod species. Each dot represents the variation in aggregate abundance between T_0 and T_f divided by the variation between T_0 and T_f in controls. For a given experiment, the net variation is then divided by the copepod abundance (ind L^{-1}) and the duration of the incubation (in d). The figure depicts the functional traits associated to copepod species *sensu* Benedetti et al. (2015).

differential sinking only whereas *in situ* collision is due to both differential sinking and turbulence (Alldredge et al., 1990; Riebesell, 1991; Jiang and Osborn, 2004; Jackson, 2015). Different feeding behavior of copepods may create at least two types

of turbulence. When filtering, copepods generate double shear field (Strickler, 1982) and thus induce micro circulation on the order of 1 to 18 mm s^{-1} (Kiørboe, 1997; Jiang and Kiørboe, 2011b). Moreover, copepod swimming behavior when foraging such as jump and swimming phases of ambush feeders create wake vortex with velocity of 240 mm s^{-1} (Kiørboe, 1997; Jiang and Kiørboe, 2011a,b). In our study the two suspension feeders (*A. clausi* and *C. helgolandicus*) we used did not promote aggregation. By comparison, in Experiments 1 and 2, activity of the small cruise feeder *E. acutifrons* induced aggregation. This suggests that turbulences created by filtering activity only were not enough to promote collisions whereas turbulence induced by small cruise feeder behavior (Strickler, 1982; Kiørboe, 1997; Jiang and Kiørboe, 2011b) seemed to favor cell collisions without disrupting coagulation. Possibly, turbulences created by larger cruise feeder such as *C. helgolandicus* may be too strong and prevent the coagulation of the cells by providing too much energy. Future studies focusing on microfluidic disturbance generated by copepod feeding and foraging are required to highlight the effects on coagulation process, and therefore confirm this statement. Collision rates are additionally related to the amount of particles in the tank (Jackson, 2015). In comparison to *E. acutifrons*, the lower aggregate abundance formed in the presence of *C. helgolandicus* could be related to its higher ingestion rates (**Table 4**). By increasing particle abundance and the differential sinking velocity, we expected that the fecal pellets produced would have increased collision rates (Burd and Jackson, 2009). This was much anticipated as fecal pellets sink much faster than free cells (100–200 vs. 1–5 m d^{-1} for fecal

FIGURE 8 | Influence of prey to predator size ratios (expressed as ESD) on aggregate dynamics: the net variation of aggregate abundance (agg ind^{-1} d^{-1}) is correlated to prey to predator size ratios (average aggregate ESD/copepod ESD). Each point represents one rolling tank. Gray shading corresponds to 99% confidence interval of the linear regression. ***p-value < 0.001 of Spearman's rho rank correlation test.
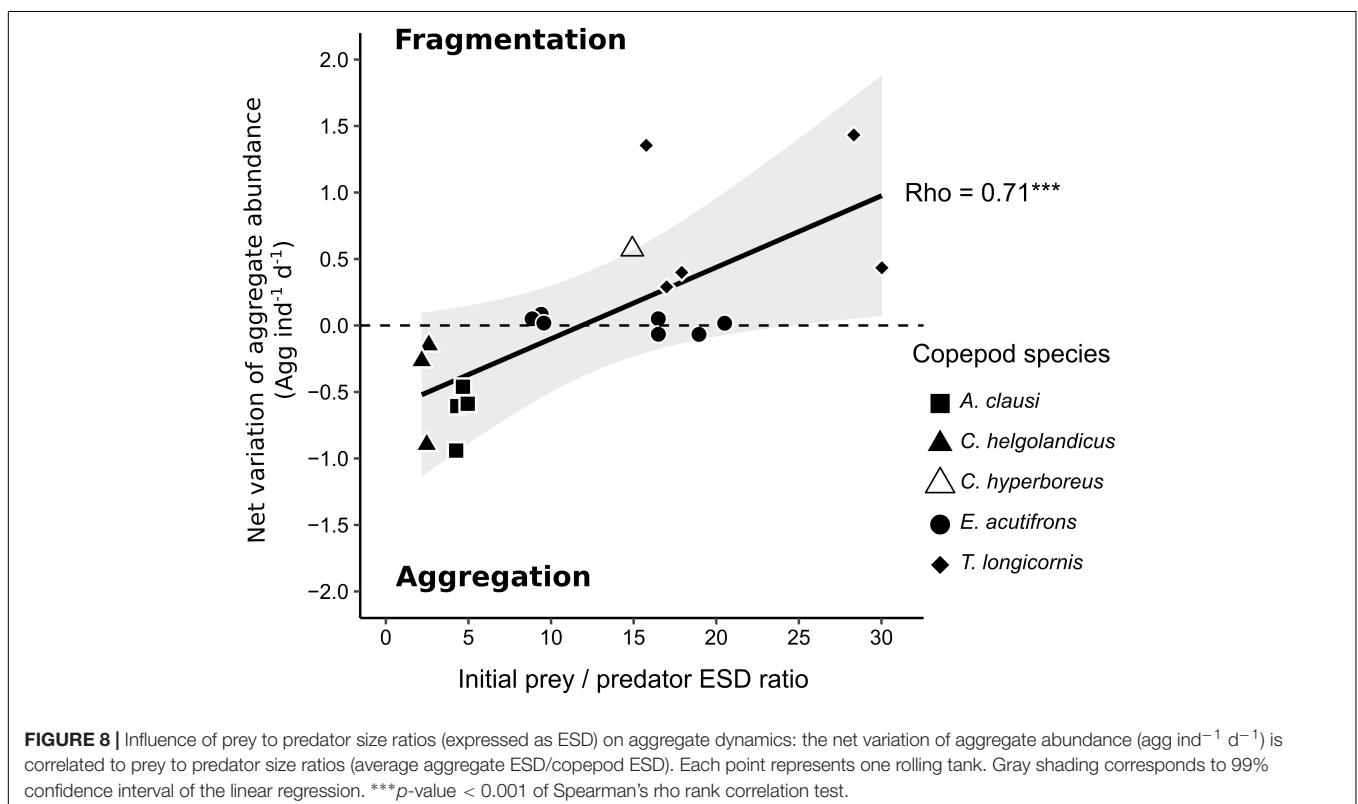
pellets and free cells, respectively; Yoon et al., 2001; Bienfang, 1981; Turner, 2015). Our set up did not allow to directly observe if fecal pellets got trapped into the aggregates formed but despite *C. helgolandicus* producing large ($145 \pm 25 \, \mu m$) and abundant fecal pellets (190–1528 per tank) no significant change in aggregate formation was evidenced. Therefore, the increase in particle abundance related to fecal pellet production did not compensate aggregate fragmentation linked to copepod grazing (i.e., increase in turbulence and decrease in cell concentration). Another process possibly affecting the collision rate is a modification of the size of the TEP. In fact, copepods do not actively feed on TEP, but could passively influence TEP size spectra by increasing the coagulation of small TEP into larger ones (Prieto et al., 2001). Turbulences due to swimming might induce TEP formation (Schuster and Herndl, 1995). Additionally, TEP size might be increased when TEP are caught into the feeding current, compacted by feeding appendages and rejected after capture (Young et al., 1997). In our study, we can hypothesize that by manipulating TEP with their feeding appendages, copepods may have contributed to increase the likelihood of collision between TEP, diatoms, and fecal pellets. However, to verify such a hypothesis required to use the microscopic TEP assay method to quantify TEP (Passow and Alldredge, 1995a; Mari et al., 2005).

Overall, our results are consistent with what was observed in a mesocosm study conducted in Norway (Moriceau et al., 2018). During this study, phytoplankton aggregation increased with copepod abundance when cyanobacteria were the dominant species. However, when diatoms constituted the bulk of the phytoplankton community, the net impact of copepods on carbon export was negative, suggesting that in this particular case, the balance between aggregation and fragmentation was in favor of particle fragmentation.

Second Set of Experiments: Implications of Grazing and Swimming of Copepods on Aggregate Characteristics

The influence of copepod grazing on aggregate size and abundance after 24 h incubation could be the result of either their direct grazing on aggregates or of their swimming activity while foraging. Similar studies were carried out with zooplankton and marine snow inside rolling tanks (Bochdansky and Herndl, 1992; Bochdansky et al., 1995). For instance, Bochdansky and Herndl (1992) showed that *A. clausi* does not significantly feed on marine snow, and concluded that the major fraction of free-living filter feeders are unable to use phytoplankton when embedded in a mucoid matrix. On the contrary, quantitative ingestion rates measured here on the four copepod species (including *A. clausi*) clearly evidenced an active grazing on diatoms even when embedded in aggregates. Direct feeding on aggregates was observed for *E. acutifrons* (see **Supplementary Video S1**) increase in gut content could not exclude feeding on both aggregate fragments and disaggregated diatoms. However, we assume the latter negligible since free diatoms were not visible when checking the incubation media *via* microscopy. Trophic interactions between zooplankton and phytoplankton aggregates were also demonstrated for protists (Artolozaga et al.,

2002), euphausiids (Dilling and Brzezinski, 2004), copepods, appendicularians, and doliolids (Taucher et al., 2018), but the process involved remain unknown.

Changes in aggregate structure were explored as a possible pathway for copepods to influence the particle flux. We hypothesized that zooplankton may change the aggregate density by repackaging or increasing Si:C ratios of the cells constituting the aggregates. First of all, in our experiments, Si:C ratios were not affected by the 24 h of grazing. Another test was through the parameters obtained from the fit of the ESD and sinking velocities data for *C. neogracile* and *S. marinoi* aggregates. Power law regressions between aggregates ESD and sinking velocity are characterized by A and B constant parameters that are comparable to those described in literature for *in situ* marine snow (Shanks, 2002; Iversen et al., 2010), with B values ranging from 0.4 to 1.3, corresponding to fractal dimensions between 1.4 and 2.3 (calculated using equation 6 from Xiao et al., 2012). In every situation where copepods fragmented the large aggregates or re-aggregated the small aggregates, the regression linking aggregate ESD and sinking velocities remained the same with unchanged A and B and so the fractal dimension D that may be derived from B (Long et al., 2015). These results suggested that copepod activities did not altered the aggregate porosity and excess density.

Particle dynamics was affected by our distinct experimental conditions regarding prey and predator types. We distinguished three different patterns: (1) fragmentation, (2) no change in the particle dynamic, and (3) re-aggregation in larger aggregates. **Figures 7**, **8** summarize re-aggregation and fragmentation patterns induced by copepods, using the variation in aggregate abundance between T_0 and T_f divided by the variation between T_0 and T_f in controls. For a given experiment, the net variation was then divided by the copepods abundance (ind L^{-1}) and the duration of the incubation (in d). **Figure 7** relates copepod functional traits to fragmentation/aggregation predominance. In **Figure 8**, we tested the impact of prey to predator size ratios onto aggregation/fragmentation balance.

Aggregate fragmentation was evidenced when a significant increase in particle abundance was associated to a decrease in their size spectra and sinking velocity. This pattern was observed for prey to predator size ratios higher than 15 (**Figure 8**) in the experiment with *T. longicornis* and *C. hyperboreus* feeding on *S. marinoi* and *Melosira* aggregates, respectively (**Table 7** and **Figures 4**, **5**, **7**, **8**). The cruise feeder *T. longicornis* was actively feeding on aggregates as also evidenced in previous experiments demonstrating the ability of *T. longicornis* to eat on sinking organic materials (Kiørboe, 2011; Lombard et al., 2013b). To our knowledge, no studies have quantified copepod ingestion while grazing on aggregates. However, our gut content values are comparable to experimental studies using phytoplankton cells as prey. We measured similar but smaller ingestion rates for *T. longicornis* in our rolling tank incubations (0.5 ± 0.3 ng Chl a_{eq} ind^{-1} d^{-1}) compared to measurements done during batch laboratory experiments (117–217 ng Chl a_{eq} ind^{-1} d^{-1}, Wang and Conover, 1986). In the experiment with *C. hyperboreus* and the natural *Melosira* sp. aggregate, videos showed that different types of interactions were at play and may explain the observed

decrease in the aggregate size. In fact, the videos evidenced that large pieces of aggregate were broken up by copepod jumping through the aggregate. Copepod swimming velocities range between 0.1 and 100 mm s^{-1} (Yamazaki and Squires, 1996) and they jump at velocities reaching up to 400 mm s^{-1} creating wake vortex with velocity of 240 mm s^{-1} (Jiang and Kiørboe, 2011a,b), which in the vicinity of fragile aggregates could be sufficient to break them. We even observed copepods hanging on aggregate before jumping, thus triggering the fragmentation of the aggregate into pieces. Interestingly when the particles were smaller and more abundant (as a result of the fragmentation), copepods swam more actively around aggregates (**Figure 6** and **Supplementary Videos S2, S3**). *C. hyperboreus* is generally considered as a passive filter feeder (Conover, 1966; Huntley, 1981; Greene, 1988). However, we observed a switch of swimming behavior from passive swept into the current when copepods were incubated with one large aggregate to active cruising when the aggregates became smaller and more numerous (as described in Strickler, 1982; Kiørboe et al., 2018). This change in their feeding foraging strategy may explain why fragmentation accelerated after 48 h (**Figure 5**). Overall, the more aggregates are fragmented, the more small aggregate abundance increases and the more copepods increase fragmentation, as can be seen from the exponential increase in aggregate abundance over time (**Figure 5**). *C. hyperboreus* seemed to be more active when aggregates ESD decreased during this experiment, suggesting that they may feed more on fragments than on whole aggregates.

Active feeding evidenced by ingestion rates in the range of 2.6 ± 0.9 to 4 ± 1 ng Chl a$_{eq}$ ind^{-1} d^{-1} is congruent with the direct feeding on whole aggregates evidenced *via* video recording (**Supplementary Video S1**). However, no changes in the *S. marinoi* and *C. neogracile* aggregate size or abundance have been observed with *E. acutifrons* (**Table 7** and **Figures 3, 4, 7, 8**). Cruise feeders detritivores (such as *E. acutifrons*) feeding on marine snow has already been demonstrated (Koski et al., 2005, 2007, 2017) and is often associated to particle flux attenuation. However in our study, *E. acutifrons* with prey to predator size ratios ranging from 7 to 20 did not significantly change the particle spectra neither in size nor in abundance or sinking rates (**Figure 8**). These results suggest that measuring grazing on aggregates is not sufficient on its own to conclude on flux attenuation.

Re-aggregation implies a decrease of aggregate abundance and an increase of the aggregate size compared to controls. This was observed for the experiments with *A. clausi* and *C. helgolandicus* feeding on *C. neogracile* and *S. marinoi* aggregates (**Figures 7, 8**). **Figures 7, 8** tend to suggest that aggregation processes prevailed over disaggregation for prey to predator size ratios lower than 6 and/or when filter feeders are predators. We believe that this pattern may be explained by the small sizes of the aggregates tested (Initial ESD = 1.9 mm in incubation with *A. clausi* and *C. helgolandicus* vs. 9 mm for the incubations with *T. longicornis* and 34 mm for *C. hyperboreus*). Small aggregates are more resistant to shear than large aggregates (Jackson, 1990), at a given shear (as induced by copepod swimming) aggregation may be facilitated between small aggregates. Reversely bigger and more fragile aggregates may be broken by the same shear

(Jackson, 1990). Unfortunately due to the impossibility to stabilize aggregate at a given size we couldn't test this hypothesis by incubating large aggregates with filter feeders and small aggregates with cruise feeders.

CONCLUSION

Our work suggested that the ability to predict the consequences of copepod activity on particle dynamic could necessitate better understanding of copepod functional traits. The general trend emerging from our study was that in the surface layer aggregation of freely suspended cells or small aggregates may be facilitated by the turbulence resulting from active swimming of small copepods. However, aggregates are fragile and their formation may be prevented by stronger turbulences as those created by larger cruise feeder copepods. As they grow in size, aggregates become more vulnerable to breakage and the same shear that was favoring aggregation of freely suspended cells (swimming of cruise feeders) or even of small aggregates preferentially fragment bigger aggregates. The main difficulty in testing this hypothesis is to stabilize aggregate at a given size in rolling tanks. While we also observed a slight increase in the diatom TEP production, our experimental set up, both in duration and in chemical analysis did not permitted to conclude on this matter. Indeed, we only measured the total pool of >0.4 µm TEP, and not the chemical composition, such as the proportion of sulfate half ester groups that may be responsible for most chemical bridges leading to aggregation (Mopper et al., 1995; Passow, 2002). We could not link either zooplankton activity to TEP size spectra which would only have been possible *via* microscopical measurements of the Alcian blue-stained TEP.

Our work may help to better understand the mechanisms driving the biological pump of carbon. Considering that carbon is efficiently isolated from the atmosphere at a depth approaching 1000 m, many recent studies start differentiating between the export efficiency and the transfer efficiency (Henson et al., 2012; Maiti et al., 2013; Cavan et al., 2017). The first is the amount of carbon produced in surface reaching the export depth (100–200 m) while the second is the proportion of the exported carbon reaching the sequestration depth. Large-scale observations suggested that ecosystems with high export efficiency such as high latitude ecosystems dominated by diatoms have a low transfer efficiency (Maiti et al., 2013). Reversely ecosystems with low export efficiency have high transfer efficiency (Henson et al., 2012; Guidi et al., 2015). Considering that aggregation of freely suspended cells and small aggregates are favored by copepod feeding activity while big aggregates are preferentially fragmented, this mechanisms may partly explained the discrepancy observed between diatoms dominated ecosystems and low productive ecosystem. Diatoms ecosystems tend to form bigger aggregates that may be exported very fast (Alldredge and Gotschalk, 1989; Cisternas-Novoa et al., 2015) but are more vulnerable to breakage by the turbulences created when copepods are feeding. Reversely, ecosystems dominated by cyanobacteria tend to form smaller aggregates (Cisternas-Novoa et al., 2015) that sink more slowly and may thus lead to smaller

export (Henson et al., 2012) but believing our results may be more resistant to copepods swimming activities.

DATA AVAILABILITY STATEMENT

The raw data supporting the conclusions of this article will be made available by the authors, without undue reservation, to any qualified researcher.

AUTHOR CONTRIBUTIONS

FUNDING

ACKNOWLEDGMENTS

SUPPLEMENTARY MATERIAL

The Supplementary Material for this article can be found online at: https://www.frontiersin.org/articles/10.3389/fmars.2019.00751/full#supplementary-material

VIDEO S1 | Copepod (*E. acutifrons*) eating on diatom aggregate (*C. neogracile*).

VIDEO S2 | *Melosira* sp. aggregate fragmentation due to copepod jump (*C. hyperboreus*).

VIDEO S3 | *Melosira* sp. aggregate fragmentation during the 72 h of incubation.

REFERENCES

Agustí, S., González-Gordillo, J. I., Vaqué, D., Estrada, M., Cerezo, M. I., Salazar, G., et al. (2015). Ubiquitous healthy diatoms in the deep sea confirm deep carbon injection by the biological pump. *Nat. Commun.* 6:7608. doi: 10.1038/ncomms8608

Alldredge, A. L., Gorsky, G., Youngbluth, M., and Deibel, D. (2005). "The contribution of discarded appendicularian houses to the flux of particulate organic carbon from oceanic surface waters," in: *Response of Marine Ecosystems to Global Change: Ecological Impact of Appendicularians*, eds G. Gorsky, M. Youngbluth, and D. Deibel (Paris: GB Science Publishers-Editions Scientifiques), 309–326.

Alldredge, A. L., and Gotschalk, C. (1988). In situ settling behavior of marine snow. *Limnol. Oceanogr.* 33, 339–351. doi: 10.1016/j.scitotenv.2016.09.115

Alldredge, A. L., and Gotschalk, C. (1989). Direct observations of the mass flocculation of diatom blooms: characteristics, settling velocities and formation of diatom aggregates. *Deep Sea Res. Part A. Oceanogr. Res. Pap.* 36, 159–171. doi: 10.1016/0198-0149(89)90131-90133

Alldredge, A. L., Gotschalk, C., Passow, U., and Riebesell, U. (1995). Mass aggregation of diatom blooms: insights from a mesocosm study. *Deep Sea Res. Part II Top. Stud. Oceanogr.* 42, 9–27. doi: 10.1016/0967-0645(95)00002-8

Alldredge, A. L., Granata, T. C., Gotschalk, C., and Dickey, T. D. (1990). The physical strength of marine snow and its implications for particle disaggregation in the ocean. *Limnol. Oceanogr.* 35, 1415–1428. doi: 10.4319/lo.1990.35.7.1415

Alldredge, A. L., and Silver, M. W. (1988). Characteristics, dynamics and significance of marine snow. *Prog. Oceanogr.* 20, 41–82. doi: 10.1016/0079-6611(88)90053-90055

Amato, A., Sabatino, V., Nylund, G. M., Bergkvist, J., Basu, S., Andersson, M. X., et al. (2018). Grazer-induced transcriptomic and metabolomic response of the chain-forming diatom *Skeletonema marinoi. ISME J.* 12, 1594–1604. doi: 10.1038/s41396-018-0094-0

Aminot, A., and Kérouel, R. (2004). *Hydrologie Des Écosystèmes Marins: Paramètres Et Analyses*. Versailles: Editions Quae.

Andersen, V., Devey, C., Gubanova, A., Picheral, M., Melnikov, V., Tsarin, S., et al. (2004). Vertical distributions of zooplankton across the Almeria–Oran frontal zone (Mediterranean Sea). *J. Plankton Res.* 26, 275–293. doi: 10.1093/plankt/fbh036

Andersen, V., Gubanova, A., Nival, P., and Ruellet, T. (2001). Zooplankton community during the transition from spring bloom to oligotrophy in the open NW mediterranean and effects of wind events. 2. vertical distributions and migrations. *J. Plankton Res.* 23, 243–261. doi: 10.1093/plankt/23.3.243

Artolozaga, I., Valcárcel, M., Ayo, B., Latatu, A., and Iriberri, J. (2002). Grazing rates of bacterivorous protists inhabiting diverse marine planktonic microenvironments. *Limnol. Oceanogr.* 47, 142–150. doi: 10.4319/lo.2002.47.1.0142

Bach, L. T., Stange, P., Taucher, J., Achterberg, E. P., Algueró-Muñiz, M., Horn, H., et al. (2019). The influence of plankton community structure on sinking velocity and remineralization rate of marine aggregates. *Glob. Biogeochem. Cycles* 33, 971–994. doi: 10.1029/2019GB006256

Beauvais, S., Pedrotti, M. L., Egge, J., Iversen, K., and Marrasé, C. (2006). Effects of turbulence on TEP dynamics under contrasting nutrient conditions: implications for aggregation and sedimentation processes. *Mar. Ecol. Prog. Ser.* 323, 47–57. doi: 10.3354/meps323047

Benedetti, F., Gasparini, S., and Ayata, S. D. (2015). Identifying copepod functional groups from species functional traits. *J. Plankton Res.* 38, 159–166. doi: 10.1093/plankt/fbv096

Berggreen, U., Hansen, B., and Kiørboe, T. (1988). Food size spectra, ingestion and growth of the copepodAcartia tonsa during development: implications for determination of copepod production. *Mar. Biol.* 99, 341–352. doi: 10.1007/BF02112126

Bergkvist, J., Klawonn, I., Whitehouse, M. J., Lavik, G., Brüchert, V., and Ploug, H. (2018). Turbulence simultaneously stimulates small- and large-scale CO 2 sequestration by chain-forming diatoms in the sea. *Nat. Commun.* 9:3046. doi: 10.1038/s41467-018-05149-w

Bergkvist, J., Thor, P., Jakobsen, H. H., Wängberg, S.-A., and Selander, E. (2012). Grazer-induced chain length plasticity reduces grazing risk in a marine diatom. *Limnol. Oceanogr.* 57, 318–324. doi: 10.4319/lo.2012.57.1.0318

Bienfang, P. K. (1981). Sinking rates of heterogeneous, temperate phytoplankton populations. *J. Plankton Res.* 3, 235–253. doi: 10.1093/plankt/3.2.235

Bochdansky, A. B., and Herndl, G. J. (1992). Ecology of amorphous aggregations (marine snow) in the Northern Adriatic Sea. 111. Zooplankton interactions with marine snow. *Mar. Ecol. Prog. Ser.* 87, 135–146. doi: 10.3354/meps087135

Bochdansky, A. B., Puskaric, S., and Herndl, G. J. (1995). Influence of zooplankton grazing on free dissolved enzymes in the sea. *Mar. Ecol. Prog. Ser.* 121, 53–63. doi: 10.3354/meps121053

Bode, M., Koppelmann, R., Teuber, L., Hagen, W., and Auel, H. (2018). Carbon budgets of mesozooplankton copepod communities in the Eastern Atlantic Ocean-regional and vertical patterns between 24°N and 21°S. *Glob. Biogeochem. Cycles* 32, 840–857. doi: 10.1029/2017GB005807

Boersma, M., Wesche, A., and Hirche, H.-J. (2014). Predation of calanoid copepods on their own and other copepods' offspring. *Mar. Biol.* 161, 733–743. doi: 10.1007/s00227-013-2373-2377

Bollens, S. M., and Frost, B. W. (1989a). Predator-induced diet vertical migration in a planktonic copepod. *J. Plankton Res.* 11, 1047–1065. doi: 10.1093/plankt/11.5.1047

Bollens, S. M., and Frost, B. W. (1989b). Zooplanktivorous fish and variable diel vertical migration in the marine planktonic copepod *Calanus pacificus. Limnol. Oceanogr.* 34, 1072–1083. doi: 10.4319/lo.1989.34.6.1072

Bollens, S. M., and Frost, B. W. (1991). Diel vertical migration in zooplankton: rapid individual response to predators. *J. Plankton Res.* 13, 1359–1365. doi: 10.1093/plankt/13.6.1359

Bollens, S. M., and Stearns, D. E. (1992). Predator-induced changes in the diel feeding cycle of a planktonic copepod. *J. Exp. Mar. Biol. Ecol.* 156, 179–186. doi: 10.1016/0022-0981(92)90244-90245

Bonnet, D., Titelman, J., and Harris, R. (2004). Calanus the cannibal. *J. Plankton Res.* 26, 937–948. doi: 10.1093/plankt/fbh087

Boyd, P. W., and Trull, T. W. (2007). Understanding the export of biogenic particles in oceanic waters: is there consensus? *Prog. Oceanogr.* 72, 276–312. doi: 10.1016/j.pocean.2006.10.007

Brierley, A. S. (2014). Diel vertical migration. *Curr. Biol.* 24, R1074–R1076. doi: 10.1016/j.cub.2014.08.054

Burd, A. B., and Jackson, G. A. (2009). Particle aggregation. *Ann. Rev. Mar. Sci.* 1, 65–90.

Capriulo, G. M., Smith, G., Troy, R., Wikfors, G. H., Pellet, J., and Yarish, C. (2002). The planktonic food web structure of a temperate zone estuary, and its alteration due to eutrophication. *Nutr. Eutrophicat. Estuar. Coast. Waters* 445, 263–333. doi: 10.1007/978-94-017-2464-7_23

Cavan, E. L., Giering, S. L. C., Wolff, G. A., Trimmer, M., and Sanders, R. (2018). Alternative particle formation pathways in the eastern tropical north pacific's biological carbon pump. *J. Geophys. Res.* 123, 2198–2211. doi: 10.1029/2018JG004392

Cavan, E. L., Henson, S. A., Belcher, A., and Sanders, R. (2017). Role of zooplankton in determining the efficiency of the biological carbon pump. *Biogeosciences* 14, 177–186. doi: 10.5194/bg-14-177-2017

Cavan, E. L., Moigne, F. A. C. L., Poulton, A. J., Tarling, G. A., Ward, P., Daniels, C. J., et al. (2015). Attenuation of particulate organic carbon flux in the Scotia Sea, Southern Ocean, is controlled by zooplankton fecal pellets. *Geophys. Res. Lett.* 42, 821–830. doi: 10.1002/2014GL062744

Chandrasekaran, R., Barra, L., Carillo, S., Caruso, T., Corsaro, M. M., Dal Piaz, F., et al. (2014). Light modulation of biomass and macromolecular composition of the diatom *Skeletonema marinoi. J. Biotechnol.* 192, 114–122. doi: 10.1016/j.jbiotec.2014.10.016

Cisternas-Novoa, C., Lee, C., and Engel, A. (2015). Transparent exopolymer particles (TEP) and Coomassie stainable particles (CSP): differences between their origin and vertical distributions in the ocean. *Mar. Chem.* 175, 56–71. doi: 10.1016/j.marchem.2015.03.009

Cisternas-Novoa, C., Lee, C., Tang, T., de Jesus, R., and Engel, A. (2019). Effects of higher CO2 and temperature on exopolymer particle content and physical properties of marine aggregates. *Front. Mar. Sci.* 5:500. doi: 10.3389/fmars.2018.00500

Cole, M., Lindeque, P. K., Fileman, E., Clark, J., Lewis, C., Halsband, C., et al. (2016). Microplastics alter the properties and sinking rates of zooplankton faecal pellets. *Environ. Sci. Technol.* 50, 3239–3246. doi: 10.1021/acs.est.5b05905

Conover, R. J. (1966). Assimilation of organic matter by zooplankton. *Limnol. Oceanogr.* 11, 338–345. doi: 10.4319/lo.1966.11.3.0338

Conover, R. J., Durvasula, R., Roy, S., and Wang, R. (1986). Probable loss of chlorophyll-derived pigments during passage through the gut of zooplankton, and some of the consequences. *Limnol. Oceanogr.* 31, 878–886. doi: 10.4319/lo.1986.31.4.0878

Conway, D. V. P. (2006). *Identification of the Copepodite Developmental Stages of Twenty-Six North Atlantic Copepods.* Plymouth: Marine Biological Association of the United Kingdom.

Conway, H. L., Harrison, P. J., and Davis, C. O. (1976). Marine diatoms grown in chemostats under silicate or ammonium limitation. II. Transient response of Skeletonema costatum to a single addition of the limiting nutrient. *Mar. Biol.* 35, 187–199. doi: 10.1007/bf00390940

Dagg, M. J. (1993). Sinking particles as a possible source of nutrition for the large calanoid copepod *Neocalanus cristatus* in the subarctic Pacific Ocean. *Deep Sea Res. Part I Oceanogr. Res. Pap.* 40, 1431–1445. doi: 10.1016/0967-0637(93)90121-I

Dam, H. G., and Peterson, W. T. (1988). The effect of temperature on the gut clearance rate constant of planktonic copepods. *J. Exp. Mar. Biol. Ecol.* 123, 1–14. doi: 10.1016/0022-0981(88)90105-90100

Darnis, G., Barber, D. G., and Fortier, L. (2008). Sea ice and the onshore–offshore gradient in pre-winter zooplankton assemblages in southeastern Beaufort Sea. *J. Mar. Syst.* 74, 994–1011. doi: 10.1016/j.jmarsys.2007.09.003

Darnis, G., Robert, D., Pomerleau, C., Link, H., Archambault, P., Nelson, R. J., et al. (2012). Current state and trends in canadian Arctic marine ecosystems: II. heterotrophic food web, pelagic-benthic coupling, and biodiversity. *Clim. Chang.* 115, 179–205. doi: 10.1007/s10584-012-0483-488

de Melo Júnior, M., Miyashita, L. K., Silva, N. J., Gaeta, S. A., and Lopes, R. M. (2013). Reproductive traits of *Euterpina acutifrons* in a coastal area of Southeastern Brazil. *Mar. Ecol.* 34, 363–372. doi: 10.1111/maec.12041

Denis, J., Vincent, D., Antajan, E., Vallet, C., Mestre, J., Lefebvre, V., et al. (2018). Gut fluorescence technique to quantify pigment feeding in downs herring larvae. *Mar. Ecol. Prog. Ser.* 607, 129–142. doi: 10.3354/meps12775

Díaz, E. R., Kraufvelin, P., and Erlandsson, J. (2012). Combining gut fluorescence technique and spatial analysis to determine *Littorina littorea* grazing dynamics in nutrient-enriched and nutrient-unenriched littoral mesocosms. *Mar. Biol.* 159, 837–852. doi: 10.1007/s00227-011-1860-y

Dilling, L., and Alldredge, A. L. (2000). Fragmentation of marine snow by swimming macrozooplankton: a new process impacting carbon cycling in the sea. *Deep Sea Res. Part I Oceanogr. Res. Pap.* 47, 1227–1245. doi: 10.1016/s0967-0637(99)00105-3

Dilling, L., and Brzezinski, M. A. (2004). Quantifying marine snow as a food choice for zooplankton using stable silicon isotope tracers. *J. Plankton Res.* 26, 1105–1114. doi: 10.1093/plankt/fbh103

Dilling, L., Wilson, J., Steinberg, D., and Alldredge, A. (1998). Feeding by the euphausiid *Euphausia pacifica* and the copepod *Calanus pacificus* on marine snow. *Mar. Ecol. Prog. Ser.* 170, 189–201. doi: 10.3354/meps170189

Durbin, E. G., and Campbell, R. G. (2007). Reassessment of the gut pigment method for estimating in situ zooplankton ingestion. *Mar. Ecol. Prog. Ser.* 331, 305–307.

Engel, A. (2000). The role of transparent exopolymer particles (TEP) in the increase in apparent particle stickiness (α) during the decline of a diatom bloom. *J. Plankton Res.* 22, 485–497. doi: 10.1093/plankt/22.3.485

Fernández-Méndez, M., Wenzhöfer, F., Peeken, I., Sørensen, H. L., Glud, R. N., and Boetius, A. (2014). Composition, buoyancy regulation and fate of ice algal aggregates in the central Arctic Ocean. *PLoS One* 9:e107452. doi: 10.1371/journal.pone.0107452

Fileman, E., Smith, T., and Harris, R. (2007). Grazing by *Calanus helgolandicus* and Para-*Pseudocalanus* spp. on phytoplankton and protozooplankton during the spring bloom in the Celtic Sea. *J. Exp. Mar. Biol. Ecol.* 348, 70–84. doi: 10.1016/j.jembe.2007.04.003

Frost, B. W. (1972). Effects of size and concentration of food of the particles on the feeding behavior marine planktonic copepod *Calanus Pacificus. Limnol. Oceanogr.* 17, 805–815. doi: 10.4319/lo.1972.17.6.0805

Gaonkar, C. A., and Anil, A. C. (2012). Gut fluorescence analysis of barnacle larvae: an approach to quantify the ingested food. *Estuar. Coast. Shelf Sci.* 111, 147–150. doi: 10.1016/j.ecss.2012.07.005

Gärdes, A., Iversen, M. H., Grossart, H.-P., Passow, U., and Ullrich, M. S. (2011). Diatom-associated bacteria are required for aggregation of *Thalassiosira weissflogii. ISME J.* 5, 436–445. doi: 10.1038/ismej.2010.145

Giering, S. L. C., Sanders, R., Martin, A. P., Henson, S. A., Riley, J. S., Marsay, C. M., et al. (2017). Particle flux in the oceans: challenging the steady state assumption: challenging the steady state assumption. *Glob. Biogeochem. Cycles* 31, 159–171. doi: 10.1002/2016GB005424

Goldthwait, S., Yen, J., Brown, J., and Alldredge, A. (2004). Quantification of marine snow fragmentation by swimming euphausiids. *Limnol. Oceanogr.* 49, 940–952. doi: 10.4319/lo.2004.49.4.0940

Goldthwait, S. A., Carlson, C. A., Henderson, G. K., and Alldredge, A. L. (2005). Effects of physical fragmentation on remineralization of marine snow. *Mar. Ecol. Prog. Ser.* 305, 59–65. doi: 10.3354/meps305059

González-Fernández, C., Toullec, J., Lambert, C., Le Goïc, N., Seoane, M., Moriceau, B., et al. (2019). Do transparent exopolymeric particles (TEP) affect the toxicity of nanoplastics on *Chaetoceros neogracile? Environ. Pollut.* 250, 873–882. doi: 10.1016/j.envpol.2019.04.093

Gorgues, T., Aumont, O., and Memery, L. (2019). Simulated changes in the particulate carbon export efficiency due to diel vertical migration of zooplankton in the North Atlantic. *Geophys. Res. Lett.* 46, 5387–5395. doi: 10.1029/2018gl081748

Gorsky, G., Chrétiennot-Dinet, M. J., Blanchot, J., and Palazzoli, I. (1999). Picoplankton and nanoplankton aggregation by appendicularians: Fecal pellet contents of *Megalocercus huxleyi* in the equatorial Pacific. *J. Geophys. Res.* 104, 3381–3390. doi: 10.1029/98JC01850

Grebner, W., Berglund, E. C., Berggren, F., Eklund, J., Harðardóttir, S., Andersson, M. X., et al. (2018). Induction of defensive traits in marine plankton-new copepodamide structures: New copepodamide structures. *Limnol. Oceanogr.* 64, 820–831. doi: 10.1002/lno.11077

Green, E. P., and Dagg, M. J. (1997). Mesozooplankton associations with medium to large marine snow aggregates in the northern Gulf of Mexico. *J. Plankton Res.* 19, 435–447. doi: 10.1093/plankt/19.4.435

Greene, C. H. (1988). Foraging tactics and prey-selection patterns of omnivorous and carnivorous calanoid copepods. *Hydrobiologia* 167, 295–302. doi: 10.1007/978-94-009-3103-9_29

Grossart, H.-P., Czub, G., and Simon, M. (2006). Algae–bacteria interactions and their effects on aggregation and organic matter flux in the sea. *Environ. Microbiol.* 8, 1074–1084. doi: 10.1111/j.1462-2920.2006.00999.x

Guidi, L., Gorsky, G., Claustre, H., Miquel, J. C., Picheral, M., and Stemmann, L. (2008). Distribution and fluxes of aggregates> 100 µm in the upper kilometer of the South-Eastern Pacific. *Biogeosciences* 5, 1361–1372. doi: 10.5194/bg-5-1361-2008

Guidi, L., Legendre, L., Reygondeau, G., Uitz, J., Stemmann, L., and Henson, S. A. (2015). A new look at ocean carbon remineralization for estimating deepwater sequestration: Ocean remineralization and sequestration. *Glob. Biogeochem. Cycles* 29, 1044–1059. doi: 10.1002/2014GB005063

Guidi, L., Stemmann, L., Legendre, L., Picheral, M., Prieur, L., and Gorsky, G. (2007). Vertical distribution of aggregates (> 110 µm) and mesoscale activity in the northeastern Atlantic: effects on the deep vertical export of surface carbon. *Limnol. Oceanogr.* 52, 7–18. doi: 10.4319/lo.2007.52.1.0007

Hansen, B., Bjornsen, P. K., and Hansen, P. J. (1994). The size ratio between planktonic predators and their prey. *Limnol. Oceanogr.* 39, 395–403. doi: 10.4319/lo.1994.39.2.0395

Henson, S. A., Sanders, R., and Madsen, E. (2012). Global patterns in efficiency of particulate organic carbon export and transfer to the deep ocean. *Glob. Biogeochem. Cycles* 26:GB1028. doi: 10.1029/2011GB004099

Hernández-León, S., Putzeys, S., Almeida, C., Bécognée, P., Marrero-Díaz, A., Arístegui, J., et al. (2019). Carbon export through zooplankton active flux in the Canary Current. *J. Mar. Syst.* 189, 12–21. doi: 10.1016/j.jmarsys.2018.09.002

Hillebrand, H., Dürselen, C.-D., Kirschtel, D., Pollingher, U., and Zohary, T. (1999). Biovolume calculation for pelagic and benthic microalgae. *J. Phycol.* 35, 403–424. doi: 10.1046/j.1529-8817.1999.3520403.x

Huntley, M. (1981). Nonselective, nonsaturated feeding by three calanoid copepod species in the Labrador Sea1. *Limnol. Oceanogr.* 26, 831–842. doi: 10.4319/lo.1981.26.5.0831

Irigoien, X., Head, R. N., Harris, R. P., Cummings, D., Harbour, D., and Meyer-Harms, B. (2000). Feeding selectivity and egg production of *Calanus helgolandicus* in the english channel. *Limnol. Oceanogr.* 45, 44–54. doi: 10.4319/lo.2000.45.1.0044

Iversen, M. H., Nowald, N., Ploug, H., Jackson, G. A., and Fischer, G. (2010). High resolution profiles of vertical particulate organic matter export off cape blanc, mauritania: degradation processes and ballasting effects. *Deep Sea Res. Part I Oceanogr. Res. Pap.* 57, 771–784. doi: 10.1016/j.dsr.2010.03.007

Iversen, M. H., and Poulsen, L. K. (2007). Coprorhexy, coprophagy, and coprochaly in the copepods *Calanus helgolandicus*, *Pseudocalanus elongatus*, and *Oithona similis. Mar. Ecol. Prog. Ser.* 350, 79–89. doi: 10.1021/acs.est.5b05905

Jackson, G. A. (1990). A model of the formation of marine algal flocs by physical coagulation processes. *Deep Sea Res. Part A Oceanogr. Res. Pap.* 37, 1197–1211. doi: 10.1016/0198-0149(90)90038-w

Jackson, G. A. (2015). Coagulation in a rotating cylinder: coagulation in a rotating tank. *Limnol. Oceanogr. Methods* 13:e10018. doi: 10.1002/lom3.10018

Jiang, H., and Kiørboe, T. (2011a). Propulsion efficiency and imposed flow fields of a copepod jump. *J. Exp. Biol.* 214, 476–486. doi: 10.1242/jeb.049288

Jiang, H., and Kiørboe, T. (2011b). The fluid dynamics of swimming by jumping in copepods. *J. R. Soc. Inter.* 8, 1090–1103. doi: 10.1098/rsif.2010.0481

Jiang, H., and Osborn, T. R. (2004). Hydrodynamics of copepods: a review. *Surv. Geophys.* 25, 339–370. doi: 10.1093/icb/icv051

Jin, X., Gruber, N., Dunne, J. P., Sarmiento, J. L., and Armstrong, R. A. (2006). Diagnosing the contribution of phytoplankton functional groups to the production and export of particulate organic carbon, CaCO2, and opal from global nutrient and alkalinity distributions: diagnosing phytoplankton functional groups. *Glob. Biogeochem. Cycles* 20:GB2015.

Kiørboe, T. (1997). Small-scale turbulence, marine snow formation, and planktivorous feeding. *Sci. Mar.* 61, 141–158.

Kiørboe, T. (2000). Colonization of marine snow aggregates by invertebrate zooplankton: abundance, scaling, and possible role. *Limnol. Oceanogr.* 45, 479–484. doi: 10.4319/lo.2000.45.2.0479

Kiørboe, T. (2011). How zooplankton feed: mechanisms, traits and trade-offs. *Biol. Rev.* 86, 311–339. doi: 10.1111/j.1469-185X.2010.00148.x

Kiørboe, T., Saiz, E., Tiselius, P., and Andersen, K. H. (2018). Adaptive feeding behavior and functional responses in zooplankton. *Limnol. Oceanogr.* 63, 308–321. doi: 10.1002/lno.10632

Komar, P. D., Morse, A. P., Small, L. F., and Fowler, S. W. (1981). An analysis of sinking rates of natural copepod and euphausiid fecal pellets 1. *Limnol. Oceanogr.* 26, 172–180. doi: 10.4319/lo.1981.26.1.0172

Koski, M., Boutorh, J., and de la Rocha, C. (2017). Feeding on dispersed vs. aggregated particles: the effect of zooplankton feeding behavior on vertical flux. *PLoS One* 12:e0177958. doi: 10.1371/journal.pone.0177958

Koski, M., Kiørboe, T., and Takahashi, K. (2005). Benthic life in the pelagic: aggregate encounter and degradation rates by pelagic harpacticoid copepods. *Limnol. Oceanogr.* 50, 1254–1263. doi: 10.4319/lo.2005.50.4.1254

Koski, M., Møller, E. F., Maar, M., and Visser, A. W. (2007). The fate of discarded appendicularian houses: degradation by the copepod, *Microsetella norvegica*, and other agents. *J. Plankton Res.* 29, 641–654. doi: 10.1093/plankt/fbm046

Lalande, C., Moriceau, B., Leynaert, A., and Morata, N. (2016). Spatial and temporal variability in export fluxes of biogenic matter in *Kongsfjorden. Polar Biol.* 39, 1725–1738. doi: 10.1007/s00300-016-1903-4

Lampitt, R. S., Salter, I., de Cuevas, B. A., Hartman, S., Larkin, K. E., and Pebody, C. A. (2010). Long-term variability of downward particle flux in the deep northeast Atlantic: causes and trends. *Deep Sea Res. Part II Top. Stud. Oceanogr.* 57, 1346–1361. doi: 10.1016/j.dsr2.2010.01.011

Lampitt, R. S., Wishner, K. F., Turley, C. M., and Angel, M. V. (1993). Marine snow studies in the Northeast Atlantic Ocean: distribution, composition and role as a food source for migrating plankton. *Mar. Biol.* 116, 689–702. doi: 10.1007/bf00355486

Laurenceau-Cornec, E., Trull, T. W., Davies, D. M., Bray, S. G., Doran, J., Planchon, F., et al. (2015). The relative importance of phytoplankton aggregates and zooplankton fecal pellets to carbon export: insights from free-drifting sediment trap deployments in naturally iron-fertilised waters near the Kerguelen Plateau. *Biogeosciences* 12, 1007–1027. doi: 10.5194/bg-12-1007-2015

Lombard, F., Guidi, L., and Kiørboe, T. (2013a). Effect of type and concentration of ballasting particles on sinking rate of marine snow produced by the Appendicularian *Oikopleura dioica*. *PLoS One* 8:e75676. doi: 10.1371/journal.pone.0075676

Lombard, F., Koski, M., and Kiørboe, T. (2013b). Copepods use chemical trails to find sinking marine snow aggregates. *Limnol. Oceanogr.* 58, 185–192. doi: 10.4319/lo.2013.58.1.0185

Lombard, F., and Kiørboe, T. (2010). Marine snow originating from appendicularian houses: age-dependent settling characteristics. *Deep Sea Res. Part I Oceanogr. Res. Pap.* 57, 1304–1313. doi: 10.1016/j.dsr.2010.06.008

Long, M., Moriceau, B., Gallinari, M., Lambert, C., Huvet, A., Raffray, J., and Soudant, P. (2015). Interactions between microplastics and phytoplankton aggregates: impact on their respective fates. *Mar. Chem.* 175, 39–46. doi: 10.1016/j.marchem.2015.04.003

Lópes, R. M., Dam, H. G., Aquino, N. A., Monteiro-Ribas, W., and Rull, L. (2007). Massive egg production by a salp symbiont, the poecilostomatoid copepod Sapphirina angusta Dana, 1849. *J. Exp. Mar. Biol. Ecol.* 348, 145–153. doi: 10.1016/j.jembe.2007.04.005

Mackas, D., and Bohrer, R. (1976). Fluorescence analysis of zooplankton gut contents and an investigation of diel feeding patterns. *J. Exp. Mar. Biol. Ecol.* 25, 77–85. doi: 10.1016/0022-0981(76)90077-0

Maiti, K., Charette, M. A., Buesseler, K. O., and Kahru, M. (2013). An inverse relationship between production and export efficiency in the Southern Ocean. *Geophys. Res. Lett.* 40, 1557–1561. doi: 10.1002/grl.50219

Malej, A., and Harris, R. P. (1993). Inhibition of copepod grazing by diatom exudates: a factor in the development of mucus aggregates? *Mar. Ecol. Prog. Ser.* 96, 33–42. doi: 10.3354/meps096033

Mari, X., Rassoulzadegan, F., Brussaard, C. P., and Wassmann, P. (2005). Dynamics of transparent exopolymeric particles (TEP) production by Phaeocystis globosa under N- or P-limitation: a controlling factor of the retention/export balance. *Harmful algae* 4, 895–914. doi: 10.1016/j.hal.2004.12.014

Mauchline, J. (1998). "Biology of calanoid copepods," in *The Advances in Marine Biology*, eds J. Blaxter, B. Douglas, and P. Tyler, (Cambridge, MA: Academic Press).

Mopper, K., Zhou, J., Sri Ramana, K., Passow, U., Dam, H. G., and Drapeau, D. (1995). The role of surface-active carbohydrates in the flocculation of a diatom bloom in a mesocosm. *Deep Sea Res. Part II Top. Stud. Oceanogr.* 42, 47–73. doi: 10.1016/0967-0645(95)00004-A

Moriceau, B., Garvey, M., Passow, U., and Ragueneau, O. (2007). Evidence for reduced biogenic silica dissolution rates in diatom aggregates. *Mar. Ecol. Prog. Ser.* 333, 129–142. doi: 10.3354/meps333129

Moriceau, B., Iversen, M. H., Gallinari, M., Evertsen, A.-J. O., Le Goff, M., Beker, B., et al. (2018). Copepods boost the production but reduce the carbon export efficiency by diatoms. *Front. Mar. Sci.* 5:82. doi: 10.3389/fmars.2018.00082

Norici, A., Bazzoni, A. M., Pugnetti, A., Raven, J. A., and Giordano, M. (2011). Impact of irradiance on the C allocation in the coastal marine diatom *Skeletonema marinoi* sarno and zingone. *Plant Cell Environ.* 34, 1666–1677. doi: 10.1111/j.1365-3040.2011.02362.x

Nowald, N., Iversen, M. H., Fischer, G., Ratmeyer, V., and Wefer, G. (2015). Time series of in-situ particle properties and sediment trap fluxes in the coastal upwelling filament off Cape Blanc Mauritania. *Prog. Oceanogr.* 137, 1–11. doi: 10.1016/j.pocean.2014.12.015

Orefice, I., Chandrasekaran, R., Smerilli, A., Corato, F., Caruso, T., Casillo, A., et al. (2016). Light-induced changes in the photosynthetic physiology and biochemistry in the diatom *Skeletonema marinoi*. *Algal Res.* 17, 1–13. doi: 10.1016/j.algal.2016.04.013

Pakhomov, E. A., Perissinotto, R., and McQuaid, C. D. (1996). Prey composition and daily rations of myctophid fishes in the Southern Ocean. *Mar. Ecol. Prog. Ser.* 134, 1–14. doi: 10.3354/meps134001

Parsons, T. R., Maita, Y., and Lalli, C. M. (1984). "Determination of chlorophylls and total carotenoids: spectrophotometric method," in *A Manual of Chemical and Biological Methods For Seawater Analysis*, eds T. R. Parsons, Y. Maita, and C. M. Lalli, (Oxford: Pergamon Press), 101–112.

Passow, U. (2002). Transparent exopolymer particles (TEP) in aquatic environments. *Prog. Oceanogr.* 55, 287–333. doi: 10.1016/S0079-6611(02)00138-136

Passow, U., and Alldredge, A. L. (1995a). A dye-binding assay for the spectrophotometric measurement of transparent exopolymer particles (TEP). *Limnol. Oceanogr.* 40, 1326–1335. doi: 10.4319/lo.1995.40.7.1326

Passow, U., and Alldredge, A. L. (1995b). Aggregation of a diatom bloom in a mesocosm: the role of transparent exopolymer particles (TEP). *Deep Sea Res. Part II Top. Stud. Oceanogr.* 42, 99–109. doi: 10.1016/0967-0645(95)00006-C

Passow, U., and Carlson, C. (2012). The biological pump in a high CO2 world. *Mar. Ecol. Prog. Ser.* 470, 249–271. doi: 10.3354/meps09985

Passow, U., and De La Rocha, C. L. (2006). Accumulation of mineral ballast on organic aggregates. *Glob. Biogeochem. Cycles* 20:GB1013. doi: 10.1029/2005GB002579

Perissinotto, R., and Pakhomov, E. A. (1996). Gut evacuation rates and pigment destruction in the Antarctic krill *Euphausia superba*. *Mar. Biol.* 125, 47–54. doi: 10.1007/BF00350759

Perissinotto, R., and Pakhomov, E. A. (1998). The trophic role of the tunicate Salpa thompsoni in the Antarctic marine ecosystem. *J. Mar. Syst.* 17, 361–374. doi: 10.1016/S0924-7963(98)00049-49

Ploug, H., Terbrüggen, A., Kaufmann, A., Wolf-Gladrow, D., and Passow, U. (2010). A novel method to measure particle sinking velocity in vitro, and its comparison to three other in vitro methods. *Limnol. Oceanogr. Methods* 8, 386–393. doi: 10.4319/lom.2010.8.386

Pondaven, P., Gallinari, M., Chollet, S., Bucciarelli, E., Sarthou, G., Schultes, S., et al. (2007). Grazing-induced changes in cell wall silicification in a marine diatom. *Protist* 158, 21–28. doi: 10.1016/j.protis.2006.09.002

Prairie, J. C., Montgomery, Q. W., Proctor, K. W., and Ghiorso, K. S. (2019). Effects of phytoplankton growth phase on settling properties of marine aggregates. *J. Mar. Sci. Eng.* 7:265. doi: 10.3390/jmse7080265

Prieto, L., Sommer, F., Stibor, H., and Koeve, W. (2001). Effects of planktonic copepods on transparent exopolymeric particles (tep) abundance and size spectra. *J. Plankton Res.* 23, 515–525. doi: 10.1093/plankt/23.5.515

R Core Team (2017). *R: A Language and Environment for Statistical Computing*. Vienna: R Foundation for Statistical Computing. Available at: https://www.R-project.org/

Riebesell, U. (1991). Particle aggregation during a diatom bloom. II. Biological aspects. *Mar. Ecol. Prog. Ser.* 69, 281–291. doi: 10.3354/meps069281

Roman, M. R., and Rublee, P. A. (1980). Containment effects in copepod grazing experiments: a plea to end the black box approach1. *Limnol. Oceanogr.* 25, 982–990. doi: 10.4319/lo.1980.25.6.0982

Sarthou, G., Vincent, D., Christaki, U., Obernosterer, I., Timmermans, K. R., and Brussaard, C. P. (2008). The fate of biogenic iron during a phytoplankton bloom induced by natural fertilisation: impact of copepod grazing. *Deep Sea Res. Part II Top. Stud. Oceanogr.* 55, 734–751. doi: 10.1016/j.dsr2.2007.12.033

Sautour, B., and Castel, J. (1993). Feeding behaviour of the coastal copepod Euterpina acutifrons on small particles. *Cah. Biol. Mar.* 34, 239–251.

Schultes, S., Sourisseau, M., Le Masson, E., Lunven, M., and Marié, L. (2013). Influence of physical forcing on mesozooplankton communities at the Ushant tidal front. *J. Mar. Syst.* 109–110, S191–S202. doi: 10.1016/j.jmarsys.2011.11.025

Schuster, S., and Herndl, G. J. (1995). Formation and significance of transparent exopolymeric particles in the northern Adriatic Sea. *Mar. Ecol. Prog. Ser.* 124, 227–236. doi: 10.3354/meps124227

Selander, E., Jakobsen, H. H., Lombard, F., and Kiørboe, T. (2011). Grazer cues induce stealth behavior in marine dinoflagellates. *PNAS* 108, 4030–4034. doi: 10.1073/pnas.1011870108

Selander, E., Kubanek, J., Hamberg, M., Andersson, M. X., Cervin, G., and Pavia, H. (2015). Predator lipids induce paralytic shellfish toxins in bloom-forming algae. *PNAS* 112, 6395–6400. doi: 10.1073/pnas.1420154112

Shanks, A. L. (2002). The abundance, vertical flux, and still-water and apparent sinking rates of marine snow in a shallow coastal water column. *Cont. Shelf Res.* 22, 2045–2064. doi: 10.1016/s0278-4343(02)00015-8

Shanks, A. L., and Edmondson, E. W. (1989). Laboratory-made artificial marine snow: a biological model of the real thing. *Mar. Biol.* 101, 463–470. doi: 10.1007/bf00541648

Shanks, A. L., and Walters, K. (1997). Holoplankton, meroplankton, and meiofauna associated with marine snow. *Mar. Ecol. Prog. Ser.* 156, 75–86. doi: 10.3354/meps156075

Smerilli, A., Balzano, S., Maselli, M., Blasio, M., Orefice, I., Galasso, C., et al. (2019). Antioxidant and photoprotection networking in the coastal diatom *Skeletonema marinoi*. *Antioxidants* 8:154. doi: 10.3390/antiox8060154

Soudant, D., and Belin, C. (2018). *Trente Années D'observation Des Micro-Algues Et Des Toxines D'algues Sur Le Littoral*. Versailles: Editions Quae.

Stamieszkin, K., Pershing, A. J., Record, N. R., Pilskaln, C. H., Dam, H. G., and Feinberg, L. R. (2015). Size as the master trait in modeled copepod fecal pellet carbon flux. *Limnol. Oceanogr.* 60, 2090–2107. doi: 10.1002/lno.10156

Steinberg, D. K. (1995). Diet of copepods (*Scopalatum vorax*) associated with mesopelagic detritus (giant larvacean houses) in monterey bay, California. *Mar. Biol.* 122, 571–584. doi: 10.1007/bf00350679

Steinberg, D. K., and Landry, M. R. (2017). Zooplankton and the Ocean carbon cycle. *Ann. Rev. Mar. Sci.* 9, 413–444. doi: 10.1146/annurev-marine-010814-015924

Stemmann, L., Gorsky, G., Marty, J.-C., Picheral, M., and Miquel, J.-C. (2002). Four-year study of large-particle vertical distribution (0–1000m) in the NW Mediterranean in relation to hydrology, phytoplankton, and vertical flux. *Deep Sea Res. Part II Top. Stud. Oceanogr.* 49, 2143–2162. doi: 10.1016/S0967-0645(02)00032-32

Stemmann, L., Jackson, G. A., and Ianson, D. (2004). A vertical model of particle size distributions and fluxes in the midwater column that includes biological and physical processes—Part I: model formulation. *Deep Sea Res. Part I Oceanogr. Res. Pap.* 51, 865–884. doi: 10.1016/j.dsr.2004.03.001

Strickler, J. R. (1982). Calanoid copepods, feeding currents, and the role of gravity. *Science* 218, 158–160. doi: 10.1126/science.218.4568.158

Svensen, C., Egge, J. K., and Stiansen, J. E. (2001). Can silicate and turbulence regulate the vertical flux of biogenic matter? A mesocosm study. *Mar. Ecol. Prog. Ser.* 217, 67–80. doi: 10.3354/meps217067

Svensen, C., Nejstgaard, J. C., Egge, J. K., and Wassmann, P. (2002). Pulsing versus constant supply of nutrients (N, P and Si): effect on phytoplankton, mesozooplankton and vertical flux of biogenic matter. *Sci. Mar.* 66, 189–203. doi: 10.3989/scimar.2002.66n3189

Taucher, J., Stange, P., Alguero-Muñiz, M., Bach, L. T., Nauendorf, A., Kolzenburg, R., et al. (2018). In situ camera observations reveal major role of zooplankton in modulating marine snow formation during an upwelling-induced plankton bloom. *Prog. Oceanogr.* 164, 75–88. doi: 10.1016/j.pocean.2018.01.004

Tréguer, P., Bowler, C., Moriceau, B., Dutkiewicz, S., Gehlen, M., Aumont, O., et al. (2017). Influence of diatom diversity on the ocean biological carbon pump. *Nat. Geosci.* 11, 27–37. doi: 10.1038/s41561-017-0028-x

Turner, J. T. (2002). Zooplankton fecal pellets, marine snow and sinking phytoplankton blooms. *Aquat. Microb. Ecol.* 27, 57–102. doi: 10.3354/ame027057

Turner, J. T. (2015). Zooplankton fecal pellets, marine snow, phytodetritus and the ocean's biological pump. *Prog. Oceanogr.* 130, 205–248. doi: 10.1016/j.pocean.2014.08.005

Vargas, C. A., Tnnesson, K., Sell, A., Maar, M., Mller, E. F., Zervoudaki, T., et al. (2002). Importance of copepods versus appendicularians in vertical carbon fluxes in a Swedish fjord. *Mar. Ecol. Prog. Ser.* 241, 125–138. doi: 10.3354/meps241125

Veit-Köhler, G. (2005). Influence of biotic and abiotic sediment factors on abundance and biomass of harpacticoid copepods in a shallow Antarctic bay. *Sci. Mar.* 69, 135–145. doi: 10.3989/scimar.2005.69s2135

Vincent, D., and Hartmann, H. J. (2001). Contribution of ciliated microprotozoans and dinoflagellates to the diet of three copepod species in the Bay of Biscay. *Hydrobiologia* 443, 193–204.

Vincent, D., Slawyk, G., L'Helguen, S., Sarthou, G., Gallinari, M., Seuront, L., et al. (2007). Net and gross incorporation of nitrogen by marine copepods fed on 15N-labelled diatoms: methodology and trophic studies. *J. Exp. Mar. Biol. Ecol.* 352, 295–305. doi: 10.1016/j.jembe.2007.08.006

Wang, R., and Conover, R. J. (1986). Dynamics of gut pigment in the copepod *Temora longicornis* and the determination of in situ grazing rates. *Limnol. Oceanogr.* 31, 867–877. doi: 10.4319/lo.1986.31.4.0867

Warwick, R. M., and Gee, J. M. (1984). Community structure of estuarine meiobenthos. *Mar. Ecol. Prog. Ser.* 18, 97–111. doi: 10.1016/j.marpolbul.2016.06.041

Wilson, S. E., Steinberg, D. K., and Buesseler, K. O. (2008). Changes in fecal pellet characteristics with depth as indicators of zooplankton repackaging of particles in the mesopelagic zone of the subtropical and subarctic North Pacific Ocean. *Deep Sea Res. Part II Top. Stud. Oceanogr.* 55, 1636–1647. doi: 10.1016/j.dsr2.2008.04.019

Xiao, F., Li, X., Lam, K., and Wang, D. (2012). Investigation of the hydrodynamic behavior of diatom aggregates using particle image velocimetry. *J. Environ. Sci.* 24, 1157–1164. doi: 10.1016/S1001-0742(11)60960-60961

Yamazaki, H., and Squires, K. D. (1996). Comparison of oceanic turbulence and copepod swimming. *Mar. Ecol. Prog. Ser.* 144, 299–301. doi: 10.3354/meps144299

Yoon, W. D., Kim, S. K., and Han, K. N. (2001). Morphology and sinking velocities of fecal pellets of copepod, molluscan, euphausiid, and salp taxa in the northeastern tropical Atlantic. *Mar. Biol.* 139, 923–928. doi: 10.1007/s002270100630

Young, S., Palm, M., Grover, J. P., and McKee, D. (1997). How Daphnia cope with algae selected for inedibility in long- running microcosms. *J. Plankton Res.* 19, 391–397. doi: 10.1093/plankt/19.3.391

Conflict of Interest: The authors declare that the research was conducted in the absence of any commercial or financial relationships that could be construed as a potential conflict of interest.

The handling Editor declared a past co-authorship with one of the authors, BM.